ACS NANOSCIENCE Au
AN OPEN ACCESS JOURNAL OF THE AMERICAN CHEMICAL SOCIETY

pubs.acs.org/nanoau
Review

Noble Metal Plasmon–Molecular Catalyst Hybrids for Renewable Energy Relevant Small Molecule Activation

Published as part of ACS Nanoscience Au virtual special issue "Advances in Energy Conversion and Storage at the Nanoscale".

Tannu Kaushik,[▽] Suchismita Ghosh,[▽] Thinles Dolkar, Rathindranath Biswas, and Arnab Dutta*

Cite This: *ACS Nanosci. Au* 2024, 4, 273–289

Read Online

ACCESS | Metrics & More | Article Recommendations

ABSTRACT: Significant endeavors have been dedicated to the advancement of materials for artificial photosynthesis, aimed at efficiently harvesting light and catalyzing reactions such as hydrogen production and CO_2 conversion. The application of plasmonic nanomaterials emerges as a promising option for this purpose, owing to their excellent light absorption properties and ability to confine solar energy at the nanoscale. In this regard, coupling plasmonic particles with molecular catalysts offers a pathway to create high-performance hybrid catalysts. In this review, we discuss the plasmonic–molecular complex hybrid catalysts where the plasmonic nanoparticles serve as the light-harvesting unit and promote interfacial charge transfer in tandem with the molecular catalyst which drives chemical transformation. In the initial section, we provide a concise overview of plasmonic nanomaterials and their photophysical properties. We then explore recent breakthroughs, highlighting examples from literature reports involving plasmonic–molecular complex hybrids in various catalytic processes. The utilization of plasmonic materials in conjunction with molecular catalysts represents a relatively unexplored area with substantial potential yet to be realized. This review sets a strong basis and motivation to explore the plasmon-induced hot-electron mediated photelectrochemical small molecule activation reactions. Utilizing in situ spectroscopic investigations and ultrafast transient absorption spectroscopy, it presents a comprehensive template for scalable and sustainable antenna-reactor systems.

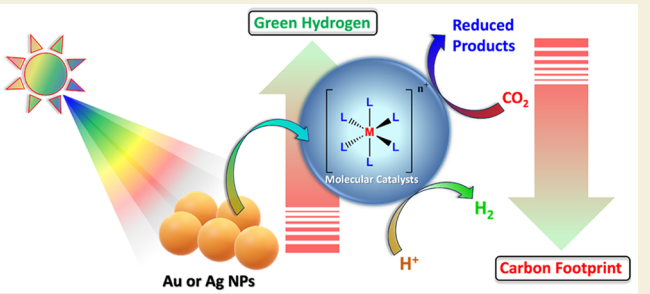

KEYWORDS: *Plasmon, Small molecule activation, Noble metal, Plasmon–molecular catalyst hybrids, Artificial photosynthesis, Hot electron utilization, Photosensitized chemical reaction, Solar energy harvesting*

INTRODUCTION

The worldwide energy system is unequivocally reliant on the consumption of fossil fuels, which accounts for a staggering 75% of the global emissions of greenhouse gases. At present, there are ongoing efforts to expedite the shift toward a sustainable and affordable clean energy platform, with the aim of mitigating climate change effects. Therefore, implementation of decarbonization strategies is vital to achieving net-zero emissions and carbon-negative goals by 2050.[1] Solar irradiation serves as the primary source of energy for the majority of the Earth's ecosystem, driving the global energy cycle. Over an entire year, approximately 342 W of solar energy falls upon every square meter of Earth. Therefore, it is one of the most abundant and easily accessible clean energy sources.[2] However, the intermittent and dilute nature of solar power necessitates its storage and portability in the form of chemical fuels or "solar fuels" to tap its full potential.[3,4] The impending global climate change can be combated by harvesting photons covering the full solar spectrum, ranging from ultraviolet (UV) to visible to near-infrared (NIR) regions, to provide a direct energy resource or to reduce atmospheric CO_2 into valuable chemical feedstocks. Hence, solar energy can play a key role in establishing an efficient carbon-neutral economy via multiple pathways.[5,6] Solar hydrogen production, as well as its subsequent storage and transportation, is another critical enabler in a paradigm shift to a decarbonized energy sector. Green hydrogen, produced through the chemical process of water splitting, is an energy-intensive, storable chemical fuel with a minimal carbon footprint. In addition, the significance of water evolution and oxygen reduction technology cannot be

Received: March 29, 2024
Revised: May 24, 2024
Accepted: May 30, 2024
Published: June 10, 2024

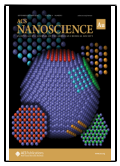

understated in the context of energy storage and conversion devices.

The intricate architectural blueprint of natural metalloenzymes has inspired the design of several biomimetic catalytic systems. Photosynthesis is fundamental in creating a balance in the carbon and oxygen cycles for driving life on the earth. It involves the absorption of sunlight by chlorophyll in a light reaction, followed by the concomitant oxidation of water to oxygen. In the dark side of this process CO_2 is reduced to carbohydrates.[7,8] This process was imitated by the appropriate combination of photocatalytic small molecule activation, where solar energy absorption by the photosensitizer generates charge-separated states. This charge separation creates the reducing and oxidizing equivalents to steer the molecular transformation at the active sites with minimal external bias while operating at ambient reaction conditions.[8] The energy input during this process can be further decreased through photoelectrocatalysis (PEC), where solar energy harvesting is performed in tandem with an applied voltage. Thus, carbon neutrality can be achieved by rationally designing artificial photosynthetic models with proper solar energy harnessing.

Hitherto, a wide range of photosensitizer-containing devices, such as dye-sensitized organic cells and perovskites with varying absorption bands and solar cells utilizing semiconductors with different band gaps, were employed for light-driven charge separation.[9−13] Albeit, these systems introduce several limitations, including photobleaching of dyes under prolonged photoexcitation, complex fabrication methods, low charge separation efficiency, and covering only a narrow solar energy spectrum <600 nm with poor energy efficiency.[14−17] Homogeneous small molecule activation reactions employ first-row transition metal-based molecular catalysts that incorporate the vital architectural features of natural metalloenzymes, light absorbers, sacrificial electron donors, and electron relay.[18] Such a bioinspired photocatalytic system facilitates real-time monitoring with *in operando* spectroscopic techniques, unravelling reaction mechanisms, and a profound understanding of the key reaction intermediates.[19] These photocatalytic models provide the template for designing photoreactors utilizing finely tuned catalysts with the desired product selectivity and reactivity. Organic dyes and molecular metal coordination complexes have been extensively investigated as efficient photosensitizers due to their strong visible-light absorption and tunable photophysical activities.[15,20,21] Nevertheless, the instability caused by their photobleaching during prolonged irradiation and the absorption of only a limited portion of the solar spectrum raise serious concerns regarding their practical applications. Later, the strategy to anchor molecular complexes covalently or noncovalently on wide and narrow band gap semiconductor surfaces has been explored in both homogeneous and heterogeneous media.[22] This material−molecular complex hybrid is a relatively robust catalytic system with extended photostability. Their improved stability is accredited to a rapid transfer of photogenerated charge carriers to molecular catalysts from the photocathode surface, enhanced recovery and reusability, and easy separation of final products. However, the narrow absorption profile of these semiconductors spanning the lower visible regions and chemical instability under harsh industrial conditions have limited their practical utility.

Recently, plasmonic gold nanomaterials have received increasing attention as photocatalysts owing to their large optical cross-section, photochemical stability, and strongly enhanced yet tunable absorbance profile, covering the majority of the solar spectrum by extending from the visible to the NIR region.[23] The optical properties of plasmonic gold nanostructures originate from the strong light absorption through the collective oscillation modes of their free electrons in the conduction band. This movement of the electrons is termed surface plasmon resonance (SPR), which presents rich opportunities for harvesting solar energy. Following the photoexcitation, surface plasmons undergo Landau damping, where plasmon resonance in the metal is damped nonradiatively into energetic charge carriers referred to as "hot electrons" and "hot holes". However, swift hot electron−hot hole recombination occurs in femtoseconds and lowers the possibility of plasmon-induced photocatalysis. Thus, in an efficient approach to utilize the hot carrier charge separation for photocatalysis, the light-harvesting-antenna plasmonic metal is combined with catalytic units through the Schottky junction. Plasmonic nanomaterials prove their mettle as photosensitizers in artificial photosynthetic systems and support the overall photocatalytic reaction, relaying the energized electrons to the immobilized catalyst. Plasmonic nanostructures are reported to be photocatalytically active for small molecule activation. However, the high energy penalty associated with these nanomaterial-driven catalyses seriously impedes their overall energy efficiency. Therefore, to overcome their limitations, plasmonic nanostructures are combined with appropriately chosen catalytic units. Wide band gap semiconductors, perovskites, MOFs, and molecular complexes are often employed as catalytic units in this strategy.[24−26] These hybrid systems improve the charge separation efficiency and utilize the photothermal and electromagnetic field enhancement properties of plasmonic nanomaterials. First-row transition metal based synthetic molecular models of enzymes have also emerged as unique catalytic systems for generating plasmon−catalyst assemblies, where they showcase high catalytic activity and selectivity.[27−29] These bioinspired complexes can be selectively tuned in terms of size, composition, and reactivity and offer controlled, easy modulation of their structural or electronic properties for targeted reactivity. Additionally, the presence of the molecular catalysts in the assembly provides an opportunity to get a glimpse of the underlying mechanism in the catalytic pathway with the deployment of suitable spectroscopic techniques. Despite the immense potential of such plasmonic-assisted molecular catalysis (PAMC), a thorough review of its application has primarily been limited to a few examples of organic transformations.[30] Here, in this review, we have expanded the horizon and discussed the use of plasmonic−molecular complex hybrids for energy-relevant small molecule activation reactions, including CO_2 reduction, hydrogen production, and water splitting. Plasmonic mediated catalysis entails thermal and nonthermal contributions from photoexcited charge carriers. This review primarily focuses on plasmon catalysis driven by photoinduced hot carrier generation and injection rather than photothermal effects activated by light-excited phonons. We shall provide a summary of various composites of plasmon-assisted molecular catalysts, in which the incorporation of plasmonic metal nanoparticles has improved reaction rates, specificity, and efficiency of product conversion through the utilization of solar energy. Our discussion will delve into the methodologies

https://doi.org/10.1021/acsnanoscienceau.4c00009
ACS Nanosci. Au 2024, 4, 273−289

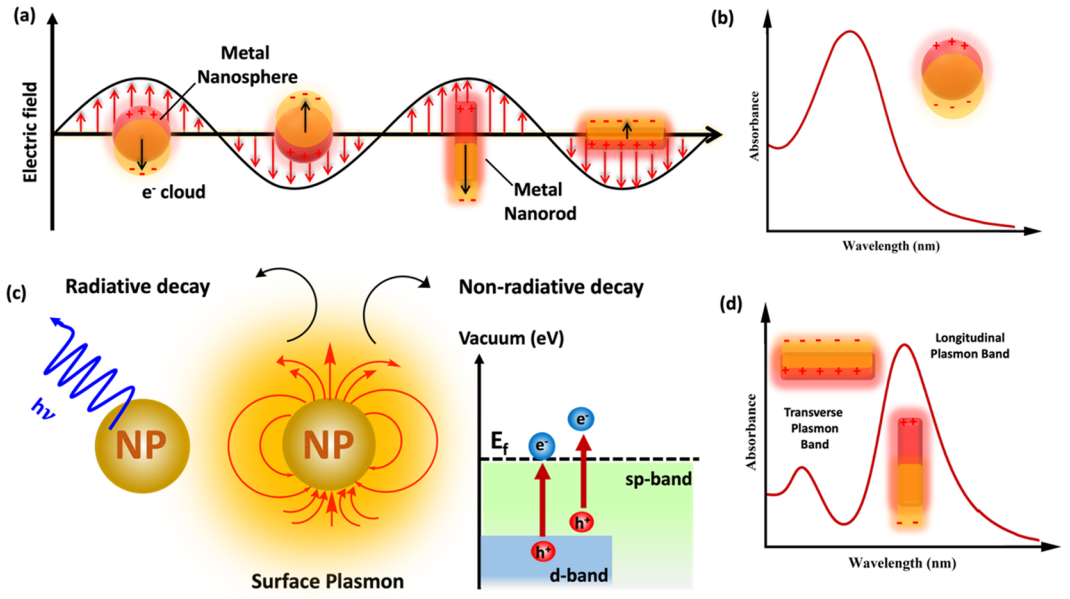

Figure 1. (a) Schematic illustration of localized surface plasmon resonance for spherical and anisotropic plasmonic metal nanoparticles. Optical extinction spectra of (b) spherical metal nanoparticles and (d) anisotropic metal nanorods under plasmonic excitation. Recreated from ref 32. Copyright 2003 American Chemical Society. (c) Surface plasmon decay occurs via both radiative and nonradiative mechanisms. This includes the emission of photons into the far-field and the nonradiative stimulation of charge carriers within the nanoparticle.

employed by researchers in this novel domain to elucidate the fundamental mechanistic routes.

PHOTOPHYSICAL PROPERTIES OF PLASMONIC NANOPARTICLES

Plasmonic nanomaterials are leading the way in the photocatalytic conversion of solar energy to chemical feedstocks. Their unique optical properties allow tunable light−matter interactions and enhanced reaction efficiencies.[31] The remarkable light-harvesting properties of plasmonic NPs are attributed to their large optical extinction cross-section, trapping of incident light in deep subwavelength regions, strong near-field enhancement, and tunable absorption in the visible to near-infrared spectral range. Metals consist of a free electron cloud plasma called a "plasmon" encircling a fixed positive atom nucleus. The surface-confined free electron cloud resonantly couples with incident light via collective coherent oscillations at a specific wavelength to give rise to the localized surface plasmon resonance (LSPR) phenomenon (Figure 1a).[31]

The strongly confined LSPR of plasmonic metal nanoparticles attributed to their sizes smaller than the wavelength of light is extensively employed for solar energy conversion, resulting in enhanced local electric field strength and efficient charge carrier creation and separation. Consequently, these noble metal nanoparticles demonstrate the "nanoantenna" effect, which is often harnessed for solar energy utilization.[34] The spectral position of the LSPR of noble metal plasmonic nanoparticles, Ag and Au, is characteristic of the extent of polarization on interaction with electrical components of incident light. Therefore, resonant conditions are determined by the particle's geometry, the dielectric constant of the metal, and the local environment.[35] A transition in the shape of AuNPs from nanospheres to asymmetric structures such as Au nanorods leads to the splitting of the SPR band into a strong and a weak band absorbing in the NIR and visible regions, respectively, similar to nanospheres.[10] The LSPR of these asymmetric AuNPs can be finely tuned to utilize a broad swath of the solar spectrum for photocatalysis (Figure 1b−d). The large optical extinction cross section (σ_{ext}) of such metal nanoparticles ascribed to their localized surface plasmon resonance is defined by the Mie approximation, as shown below. Plasmonic nanoparticles can exhibit large optical extinction cross-section on LSPR photoexcitation which is up to 10 times larger than their geometric area for spherical nanoparticles and even larger for nanoparticle clusters.[33] The extinction cross-section for spherical nanoparticles is intricately linked to the complex dielectric function of the metal, as follows:

$$\sigma_{ext} \approx \frac{\varepsilon_2}{[\varepsilon_1 + 2\varepsilon_m]^2 + \varepsilon_2^2}$$

Here, ε_1 and ε_2 are real and imaginary parts, respectively, of the dielectric function of the metal, and ε_m is the dielectric function of the medium. The LSPR in metal nanoparticles depends on the real and imaginary parts of the dielectric constant. The real part of the dielectric function (ε_1) describes the extent of polarizability of the metal with respect to wavelength and should be large and negative, whereas the imaginary part (ε_2) is supposed to be negligible and positive. The dielectric function (ε_m) for noble metals exhibits a strong correlation with the wavelength of the electromagnetic field. The physical significance of this relation can be explained such that when the denominator approaches zero, the optical extinction cross-section will be maximum; thus, $\varepsilon_1 = -2\varepsilon_m$ and ε_2 should be small for plasmonic excitation. Polarizability, the real part of the dielectric function central to the plasmonic effect of metals, is comparatively easier. Therefore, their real part is generally negative, and for many metals $\varepsilon_1 = -2\varepsilon_m$ holds true in air at UV−visible wavelengths. Therefore, size and shape of plasmonic nanoparticles can be explicitly manipulated

https://doi.org/10.1021/acsnanoscienceau.4c00009
ACS Nanosci. Au 2024, 4, 273−289

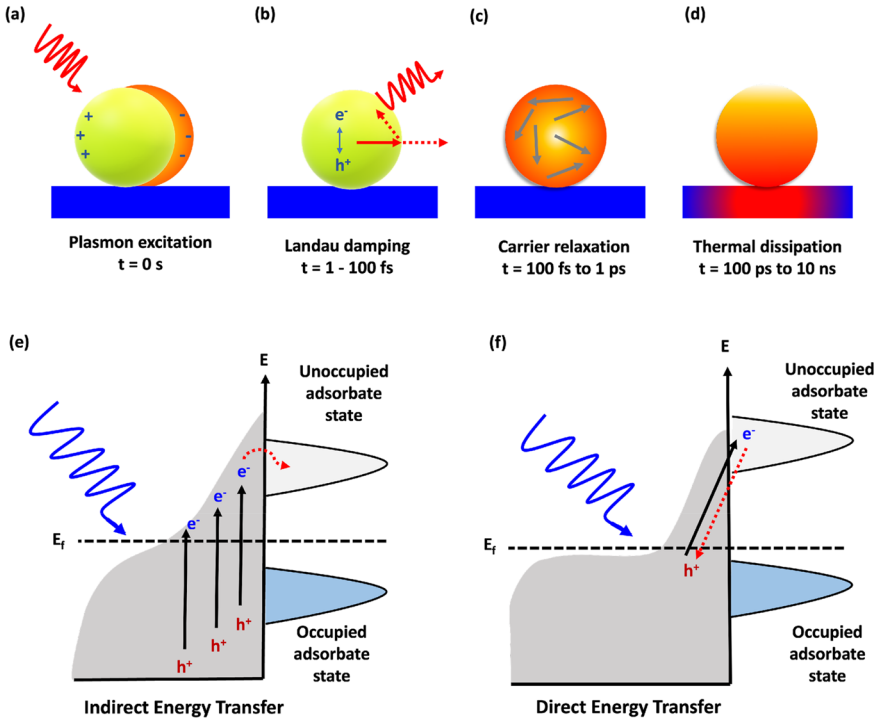

Figure 2. (a–d) Successive surface plasmon excitation and relaxation mechanisms encompassing temporal elements and the distribution of charge carriers across electronic states. (a) Excitation of a localized surface plasmon on interaction with incident photons. (b) Surface plasmons on photoexcitation undergo Landau damping (1–100 fs), wherein plasmon resonance in the metal is damped nonradiatively into energetic charge carriers referred to as "hot electrons and holes". (c) Redistribution of thermal energy among hot carriers occurs through the electron–electron scattering mechanism (time scale ∼100 fs to 1 ps). (d) Thermal dissipation to the surroundings via thermal conduction (time scale ∼100 ps to 10 ns). Schematic depiction of hot electron transfer from plasmonic nanomaterials to adsorbate molecules through (e) the indirect energy transfer pathway and (f) the direct energy transfer pathway. Recreated from ref 14. Copyright 2022 American Chemical Society.

to absorb in the visible to near-infrared regions of the broadband solar spectrum.

It is imperative to understand the charge and energy transfer dynamics involved in the excitation of reactants at plasmonic metal surfaces when exposed to light for tailoring and tuning the absorption profile and achieve optimum energy conversion efficiencies.[35] There exist two distinct forms of electronic excitation that can occur within plasmonic metal-based systems, namely, interband excitation, which involves the transition of electrons from filled d states to vacant s states situated above the Fermi level, and intraband excitation, which entails the transition of electrons from filled s states to vacant s states (Figure 1c). The intraband transitions are forbidden and thus have a low rate constant of $\sim 10^{13}$ s^{-1} and are promoted only on the change in momentum of charge carriers induced by lattice phonons and plasmons. However, interband excitation is allowed, and the absorption wavelength required for transition depends on the position of the d band below the Fermi level. The position of the d band in Ag is significantly lower in energy than the Fermi level. Hence, the d–s excitation for silver nanoparticles does not take place in the visible region. The d band of Au and Cu is much higher in energy and near the Fermi level, thus allowing the d–s excitation in the visible region. Thus, Ag, Au, and Cu having considerably small ε_2 (real part) values and $\varepsilon_1 = -2\varepsilon_m$ allow surface plasmon resonance in the visible region which can be extended to the NIR region.[36]

Strong plasmonic confinement of light energy leads to considerable electric field intensity enhancement at the interface of the metal nanoparticle surfaces, resulting in unparalleled optical extinction properties and thermal effects of the nanoparticles. Consequently, these strong light absorption properties in the visible to NIR regions have been extensively utilized in photocatalysis for small molecule activation and are known to be a potential gateway for harvesting renewable energy.[37] LSPR excitation not only harnesses solar energy but also enhances the selectivity and rate of chemical transformations, thus proving the mettle of metal nanoparticles in catalysis. These plasmonic nanomaterials can harness a broad range of the solar spectrum from visible to NIR regions; therefore, we can utilize the most abundant renewable energy resource, solar energy, directly in catalyzing reactions of utmost importance such as in carbon capture and utilization and green hydrogen production.[38−40] In an effort to reduce the greenhouse gas CO_2 in the environment, plasmonic nanomaterials can simultaneously capture solar energy and enhance the catalytic rate of molecular activation due to energetic charge carriers. LSPR on photoexcitation undergoes damping of surface plasmon resonance either radiatively or nonradiatively (Landau damping), subsequently leading to nonthermal distribution of energetic charge carriers (hot electrons and holes) (Figure 1c). The energy of these hot carriers is further redistributed in a Fermi–Dirac distribution followed by a fast hot electron–hole recombination on some order of femtoseconds with dissipation of energy thermally to the surroundings (Figure 2a–d). Following the absorption of light and subsequent photoexcitation, the dephasing stages of LSPR take place within a femtosecond time frame. Various experimental conditions have been explored through experimental and theoretical investigations to elucidate the hot-

https://doi.org/10.1021/acsnanoscienceau.4c00009
ACS Nanosci. Au 2024, 4, 273–289

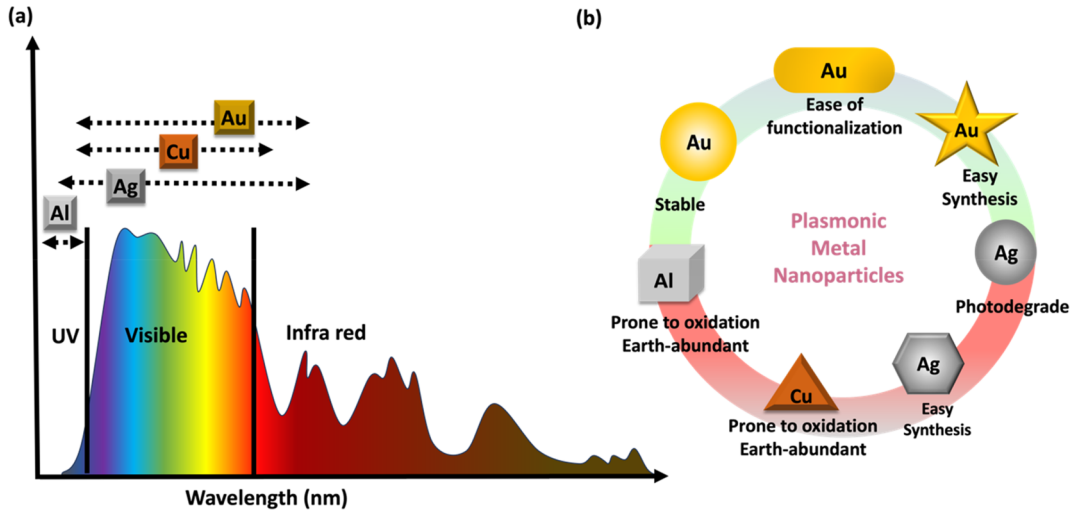

Figure 3. (a) Summary of predominant absorption spectral ranges of different plasmonic metals for utilization of broadband solar spectrum by different shapes and sizes of metal nanoparticles. Gold (Au) primarily absorbs in the visible (520−550 nm) range and exhibits significant optical response in the NIR region (700−1000 nm) with precisely engineered anisotropic nanostructures. Silver (Ag) typically absorbs and scatters in the UV−visible region (400−500 nm) and has limited NIR absorption on modifications. Nonprecious metals: Aluminum (Al) absorbs in the UV region (200−300 nm) with weak and broad absorption extending into the Vis−NIR range for different shape and size nanoparticles. Copper (Cu) harnesses the full visible region of the solar spectrum and conventionally not employed in absorption in the NIR region due to poor stability. (b) Schematic drawing comparing characteristic optical and physical properties of noble and nonprecious plasmonic metal nanoparticles.

carrier dynamics driving the desired chemical reaction. Nonetheless, a pressing requirement remains to distinguish the specific energy transfer mechanisms contributing to plasmonic enhancement. These mechanisms may include plasmon-induced injection of hot electrons, plasmon-induced resonance energy transfer, plasmon-induced re-emission of photons (radiative energy transfer), as well as direct electron injection to the adsorbate.[10,41] The molecular activation by energetic hot carriers at the metal−molecule interface is presumed to follow either a direct or indirect pathway. In the indirect energy transfer pathway, hot carriers of appropriate energy are transferred to the lowest unoccupied molecular orbital of the reactants adsorbed on the metal surface, which leads to nonthermal activation of the chemical bonds of adsorbates (Figure 2e). The efficiency of indirect electron excitation from the metal to the unoccupied orbital of the reactant depends on the location of its LUMO near the Fermi energy level of the metal.[7−14] In contrast, in the direct energy transfer pathway, the metal and molecule concomitantly generate new electronic states at their interface, and the energy transfer takes place from the occupied orbitals of the composite to the unoccupied orbitals (Figure 2f). It results in chemical transformation at the interface of the complex via electronic or vibrational excitation of the adsorbates.[7−11,13] Thus, LSPR-generated energetic charge carriers can be explicitly employed for enhancing catalytic rates with a greater selectivity of the reaction upon photoirradiation of suitable wavelengths.[41−43]

Of the light that reaches the earth's surface, infrared radiation makes up 49.4%, visible light contributes 42.3%, and ultraviolet radiation constitutes slightly over 8% of solar radiation. So far, noble metal-based nanoparticles, namely, gold and silver, and nonprecious copper and aluminum have been reported to demonstrate plasmonic properties, each having exclusive plasmonic properties in different spectral ranges[43−47] (Figure 3a). Copper is an earth-abundant and inexpensive metal and, thus, a prospective alternative to the rare and expensive noble metal nanoparticles. Copper nanoparticles (CuNPs) are known for their excellent optical and catalytic properties arising from the large surface area to volume ratio and quantum confinement effects.[48] LSPR in CuNPs is observed due to interband transitions between the valence and Fermi energy levels of the copper, which could be the principal reason for the comparatively weaker resonance shift of the CuNPs. However, CuNPs are not very stable under atmospheric conditions and are prone to oxidation. Much research effort to stabilize CuNPs under air, water, and chemical environments has been reported involving complex synthetic structures.[49] Copper, being a first-row transition element, has fascinating physical and chemical properties, such as its multiple accessible oxidation states, and offers excellent catalytic properties. Optical extinction properties of plasmonic nanoparticles can be readily tuned to absorb in a wide spectrum, from the visible to NIR region. However, shifting the absorption to a higher energy region, i.e., the UV region, is comparatively more challenging. In contrast, gold nanoparticles (AuNPs) experience loss of energy via increased scattering channels for wavelengths below 550 nm due to interband transitions. Silver nanoparticles (AgNPs) are known to absorb down to 350 nm yet suffer from loss of plasmonic properties due to rapid oxidation. Aluminum has emerged as a rising star owing to its excellent plasmonic properties in the UV and visible regions of the spectrum, low cost, earth-abundance, and high compatibility with semiconductor metal oxides.[50] Nonetheless, experimental optical responses of aluminum nanoparticles (AlNPs) have been inconsistent due to the oxidation of AlNPs under atmospheric conditions, creating ambiguity due to a difference in the expected active plasmonic surface. Therefore, AlNP plasmonic resonances are sensitive to the presence of oxides within the metal. This comparison establishes AuNPs as the best possible option for photocatalyst due to their large optical cross-section, increased photostability, ability to enhance intense local electromagnetic fields within a few nanometers at the metal−dielectric

https://doi.org/10.1021/acsnanoscienceau.4c00009
ACS Nanosci. Au 2024, 4, 273−289

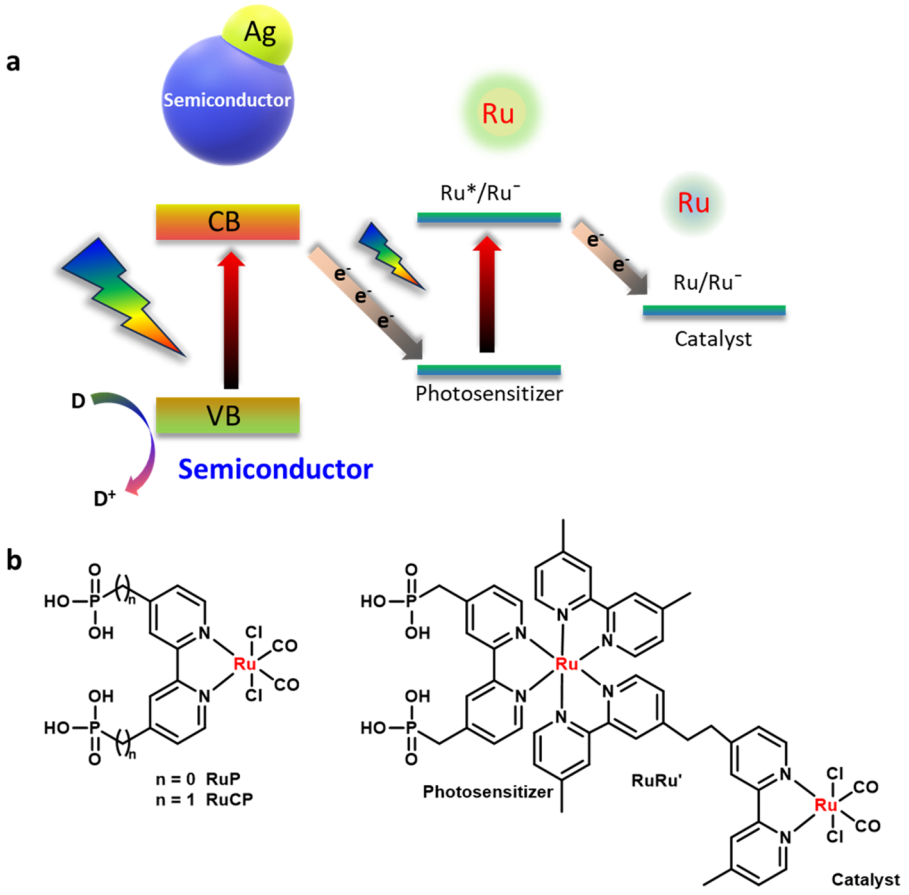

Figure 4. (a) Z-Scheme CO_2 reduction using a hybrid of a semiconductor and a binuclear Ru(II) complex. (b) Various Ru(II) complexes used by the Ishitani group[68−73] for photocatalytic CO_2RR. Adapted with permission from ref 70. Copyright 2016 American Chemical Society.

interface, and easy surface functionalization.[44] The optical absorption properties of gold nanoparticles can be simply tuned from the visible to NIR regions by modulating the shape, size, and morphology. AuNPs remain inert under atmospheric conditions. Hence, AuNPs are stable under oxygen and can be synthesized at room temperature using simple wet chemical methods. AgNPs, on the other hand, show strong plasmonic interplay with light and have the largest scattering cross-section compared to other metals.[45] Their absorption profile can be tuned from ultraviolet to visible regions by tuning their size, shape, and dielectric environment. Silver nanoparticles exhibit sharper LSPR bands and thus exhibit an optimum application in sensors. However, silver nanoparticles tend to photodegrade under prolonged visible photoexcitation.[46,47] This descriptive comparison establishes the advantages of exploiting noble metal plasmonic nanoparticles in small molecule activation reactions (Figure 3b).

PLASMONIC METAL−MOLECULAR COMPLEX HYBRIDS FOR CO_2 REDUCTION

CO_2 reduction is a multistep redox process. It starts with a one-electron reduction of a linear and chemically inert CO_2 molecule to a bent CO_2 radical anion ($CO_2^{\bullet-}$). This step is endergonic and kinetically sluggish.[51] The formation of the $CO_2^{\bullet-}$ anion is a thermodynamically uphill reaction and requires high negative potential (E° = −1.90 V vs SHE in aqueous media) due to the internal reorganization of the molecule and solvent effect.[52] Therefore, designing an efficient catalyst exhibiting high catalytic activity and selectivity is challenging in overcoming the kinetic and thermodynamic barrier associated with multistep electron reduction of CO_2 and negating the formation of mixed products. A basic understanding of the CO-dehydrogenase (CODH) enzyme, known for catalyzing CO_2 reduction to CO in nature, paved the way for designing artificial constructs that simulate the architectural blueprint of these enzymes.[53] CO_2 binding and reduction on the [NiFe] cluster of the CODH enzyme involves its activation by two metal centers and subsequent stabilization through hydrogen bonding by appropriate pendant proton donors in the outer coordination sphere.[54] Inspired by this natural and extremely effective catalyst design, continuous efforts have been put in by the scientific community to pursue efficient artificial CO_2 reduction.[55] Therefore, combining plasmonic nanomaterials with molecular catalysts is a new strategy to fabricate catalysts with high catalytic activity and selectivity. Molecular catalysts can act as functional mimics of natural metalloenzymes by incorporating unique enzymatic features in their framework.[56] They can also be selectively tuned in terms of size, composition, and reactivity, offering controlled, easy modulation of their structural or electronic properties for increased reactivity.[57] However, these metal complexes are commonly employed in homogeneous catalysis and have several demerits, such as slow charge transfer rates and tedious separation of the reaction mixtures, thus, posing difficulties in their practical applicability. The catalytic activity of such systems is typically slow, as they display turnover numbers (TON) in the range of 15−30 over a period of hours and often require elevated pressure and excess organic solvents

https://doi.org/10.1021/acsnanoscienceau.4c00009
ACS Nanosci. Au 2024, 4, 273−289

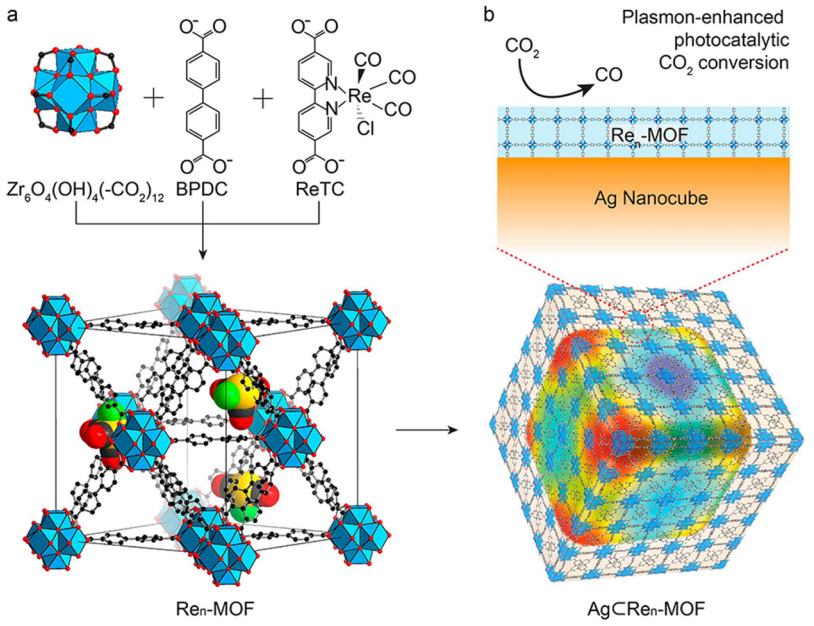

Figure 5. Structures of Re_n-MOF and Ag⊂Re_n-MOF for photocatalytic CO_2 conversion. (a) $Zr_6O_4(OH)_4(-CO_2)_{12}$ secondary building units are combined with biphenyl-4,4′-dicarboxylic acid (BPDC) and ReTC linkers to form Re_n-MOF. The structure of Re_3-MOF identified from single-crystal X-ray diffraction is shown. The 12-coordinated Zr-based metal clusters are interconnected by 21 BPDC and 3 ReTC linkers in a face-centered cubic array. Atom labeling scheme: C, black; O, red; Zr, blue polyhedra; Re, yellow; Cl, green; H atoms are omitted for clarity. (b) Re_n-MOF coated on a Ag nanocube for enhanced photocatalytic conversion of CO_2. Adapted with permission from ref 87. Copyright 2016 American Chemical Society.

to expedite the reaction. Integrating molecular complexes with plasmonic NPs resolves the above limitations, making a hybrid-type photoelectrode where the inherent tunable reactivity and selectivity of molecular complexes are complimented by efficient light harvesting and charge transfer by plasmonic materials.[58] In the past few years, the ability of such hybrids has been greatly exploited for efficient reduction of CO_2. In the following section, we will provide a concise overview of several pioneering instances where hybrids combining plasmonic nanomaterials and metal catalysts have been employed.

Hybrids of molecular catalysts and semiconductors are promising photocatalysts for CO_2 reduction.[22,59−61] Here, the inorganic/organic semiconductors act as photosensitizers, and photoexcited electrons are transferred to the molecular catalyst, enhancing the catalytic reaction.[61,62] The introduction of noble metal nanoparticles often facilitates interfacial charge transfer between semiconductors and molecular catalysts. In the following reports, we shall investigate the mechanisms by which plasmonic metal nanoparticles facilitate interfacial charge transfer via the enhancement of charge carrier generation induced by LSPR, injection of hot electrons into the conduction band of neighboring semiconductors, direct transmission of energy to semiconductors through resonant energy transfer, separation of photogenerated electrons and holes, and provision of additional catalytic sites for the reduction of CO_2 to augment the overall catalytic efficiency of CO_2 conversion.

Recently, Wang et al. studied a hybrid of $ZnIn_2S_4$ (ZIS) and the tetra(4-carboxyphenyl)porphyrin iron(III) chloride (FeTCPP) molecular catalyst for CO_2RR.[63] ZIS, with its excellent visible-light response, often exhibits low photocatalytic efficiency due to rapid charge recombination. Introducing Au/Ag nanoparticles in the mix enhances the charge separation and promotes interfacial charge transfer from ZIS to FeTCPP, boosting photocatalytic CO_2 conversion. These results reveal that appropriate loading of Ag nanoparticles can act as a promoter for interfacial electron transfer from ZIS to FeTCPP. However, excess AgNPs can aggregate and cover the active sites of the ZIS surface, hindering the redox reactions and thereby lowering the overall efficiency. In contrast to Ag, introducing Au nanoparticles decreased the selectivity toward CO production and enhanced H_2 yield, assuming the lower overpotential of Au nanoparticles for proton reduction. These hybrid catalysts showed good stability up to 9 h of illumination.

Au/TiO_2 hybrids have been extensively investigated because of their efficient light-harvesting properties and ability to generate plasmon-induced hot electrons.[64−66] In an interesting study, Nam et al. immobilized the RuCY molecular catalyst onto the Au/TiO_2 heterostructure through a stable Ti-phosphonate linkage to develop an effective photocatalyst for CO_2 conversion (Figure 4a).[67] The plasmonic Au/TiO_2 heterostructure promotes multielectron transfer toward the active catalyst through efficient charge separation at a Schottky junction, enhancing the photocatalytic activity. The hybrid system showed remarkable stability and reusability, maintaining its catalytic activity over 50 h without any loss. The abundant electron supply from the plasmonic nanostructure contributes to the remarkable selectivity toward formic acid (95%) even at low pH, as the formation of formic acid is favored when multiple electrons can be supplied simultaneously.

In an effort to develop an artificial Z-scheme system, the Ishitani group utilized a hybrid photocatalyst that consists of a supramolecular bimetallic ruthenium complex (RuBLRu′) adsorbed onto Ag-loaded TaON (Ag/TaON).[68,69] In this work, methanol is used as a reducing agent and a sacrificial electron donor. Methanol is oxidized to formaldehyde in this

https://doi.org/10.1021/acsnanoscienceau.4c00009
ACS Nanosci. Au 2024, 4, 273−289

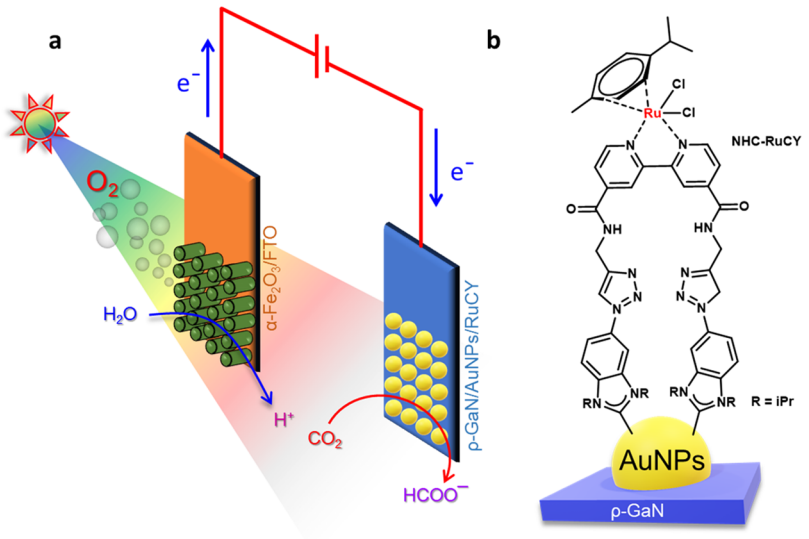

Figure 6. Schematic representation of (a) photoelectrochemical CO_2 conversion reaction on α-Fe_2O_3/fluorinated tin oxide (FTO)‖p-GaN/AuNP/RuCY and (b) immobilization of RuCY on the surface of AuNPs via the NHC ligand. Recreated with permission from ref 92. Copyright 2020 American Chemical Society.

process, and it donates two electrons that reduce CO_2 to formic acid. The Ag nanoparticles enhance the photocatalytic activity of the hybrid system by facilitating electron transfer from the valence band of TaON (tantalum oxynitride) to the excited or oxidized photosensitizer unit (Ru/Ru′) (Figure 4b). Additionally, Ag nanoparticles can act as an electron pool, enhancing the electron−hole separation in the excitation of TaON and subsequently improving the efficiency of methanol oxidation. In the overall process, light energy converts to chemical energy with ΔG° = +83.0 kJ/mol. However, the Ag/TaON system showed moderate selectivity (60%), which was further modified using metal-free graphitic carbon nitride (C_3N_4) semiconductors in their following work. Further continuing along the same line, this group successfully developed an artificial Z-scheme system that mimics natural photosynthesis.[70] In this work, the C_3N_4 semiconductor was modified by loading Ag nanoparticles and coupled with the Ru(II) binuclear complex (Ru/Ru′) to construct a RuRu′/Ag/C_3N_4 photocatalyst. This hybrid material exhibited CO_2RR activity, displaying a high turnover and selectivity for formic acid production. This catalytic assembly was efficient and durable even under aqueous conditions, despite the hydrophobic nature of C_3N_4 and the low solubility of CO_2 in water. The researchers conducted several control experiments, varying the reaction environments (argon and CO_2) and catalytic components to establish the synergy between hybrid components. Without Ru/Ru′, the selectivity for formate was greatly reduced as competitive H_2 production occurred. Interestingly, the loading of other metals, such as Au/Pt, onto C_3N_4 dominantly generated H_2. The results indicate that the key to the high efficiency and selectivity of such a hybrid system is the use of a Ag modifier that has a large overpotential for proton reduction and mediates interfacial electron transfer from C_3N_4 to the excited state of Ru/Ru′.

Later, in very similar studies, they utilized Ag-modified C_3N_4 nanosheets (NS-C_3N_4) along with a mononuclear Ru(II) complex (RuP)[71] and the binuclear RuRu′[72] to obtain visible-light-driven efficient CO_2-to-formate conversion. Very recently, they have substantially improved the catalytic performance of the hybrid by modifying the molecular complex by inserting a methylene spacer between the diamine ligand and phosphonic acid group to construct RuCP.[73] The modified hybrid RuCP/Ag/C_3N_4 demonstrated significantly increased CO_2 reduction activity with higher HCOOH yields and selectivity than those of RuP/Ag/C_3N_4. Figure 4a displays a schematic representation of the mechanism involved in the plasmonic-assisted photocatalytic process by the various ruthenium complexes (Figure 4b) utilized by their group.

There have been various studies involving photoactive metal complexes,[56,74−76] MOFs,[77−83] and inorganic nanostructures[16,84−86] with varying levels of CO_2 reduction performance. On this front, Choi et al. reported a MOF-coated nanoparticle hybrid catalyst that consists of a Re complex (ReTC) covalently attached to a zirconium MOF, UiO-67 (Figure 5).[87] The MOF unit prevents dimerization, which leads to deactivation of the molecular photocatalyst. The researchers have quantitatively controlled the density of the molecular photocatalyst in the frame to construct Re_n-MOF (n = 0, 1, 2, 3, 5, 11, 16, and 24 complexes per unit cell), and the highest activity was found for Re_3-MOF. Further incorporation onto Ag nanocubes (Ag⊂Re_3-MOF) as plasmonic enhancers increased the photocatalytic CO_2-to-CO conversion by 7-fold. On irradiation, the Ag nanocubes can generate intensified near-surface electric fields with significantly higher magnitudes than the incident electromagnetic field. As a result, the photoactive Re centers in the Re_n-MOFs are spatially localized to the intensified electric fields, leading to a significant increase in the photocatalytic activity. Additionally, the Ag⊂Re_n-MOF exhibits long-term stability, maintaining its photocatalytic performance for up to 48 h.

N-heterocyclic carbenes (NHCs) also emerged as promising candidates for surface functionalization of gold nanoparticles to develop sustainable hybrid-type photocatalysts.[88−90] In this context, Chang et al. have demonstrated that an NHC-functionalized AuNP catalyst can exhibit improved Faradaic efficiency (FE = 83%) for CO_2 reduction in water at neutral pH compared to the parent AuNP (FE = 53%).[91] Further, Jun et al. reported an example of a ruthenium molecular complex

https://doi.org/10.1021/acsnanoscienceau.4c00009
ACS Nanosci. Au 2024, 4, 273−289

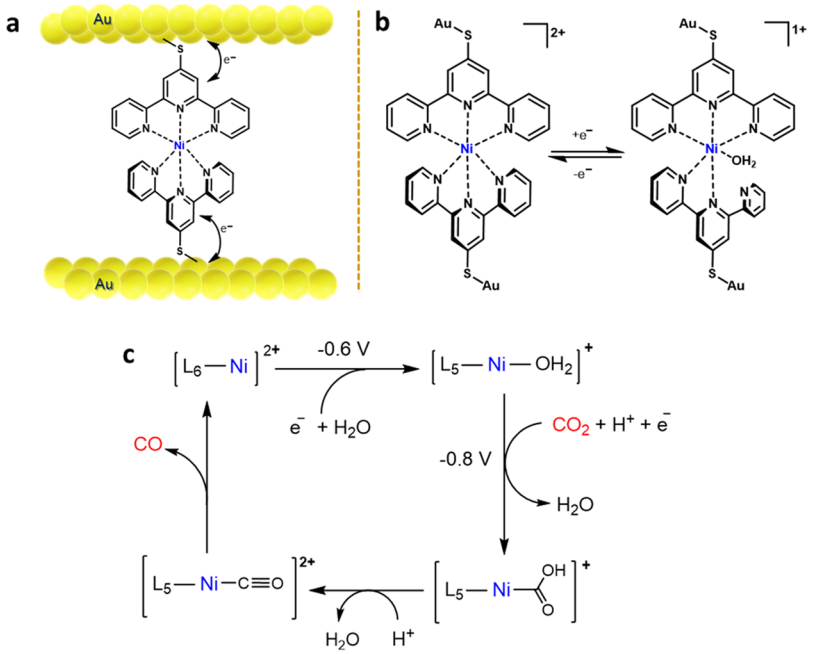

Figure 7. (a) Schematic representation of $[Ni(tpyS)_2]$ sandwiched between two Au surfaces. (b) $[Ni(tpyS)_2]^{2+}$ (at 0 V) and its one-electron reduced form $[Ni(tpyS)_2\text{-}H_2O]^{1+}$ (at −0.6 V). (c) Proposed catalytic cycle of $Ni(tpyS)_2$-mediated CO_2 reduction. L_n represents tpyS ligands forming Ni−N bonds. $[L_6{-}Ni]^{2+} = [Ni(tpyS)_2]^{2+}$, $[L_5{-}Ni{-}H_2O]^{1+} = [Ni(tpyS)_2{-}H_2O]^{1+}$ Recreated from ref 93. Copyright 2021 Springer Nature Limited.

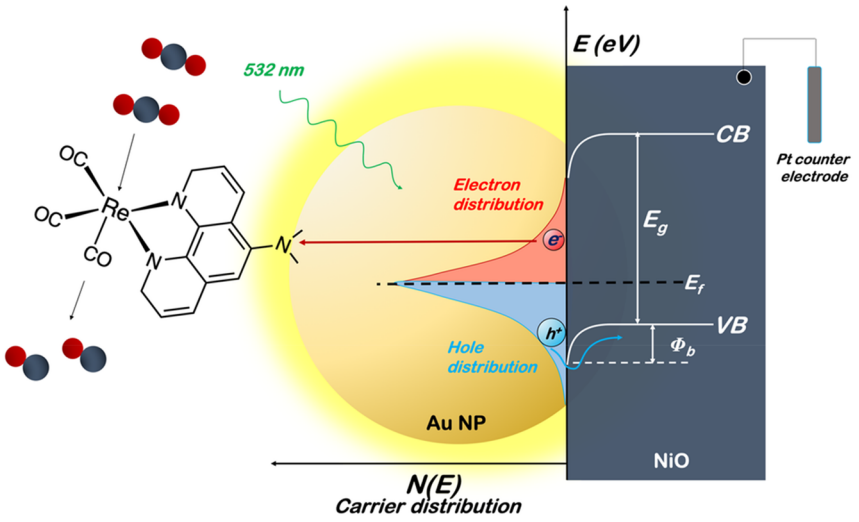

Figure 8. Schematic representation of the photoelectrocatalytic system for directly reducing CO_2 to CO with a NiO/Au/Re^I(phen-NH_2)$(CO)_3Cl$ (phen-NH_2 = 1,10-phenanthrolin-5-amine) plasmon nanohybrid system. Reproduced from ref 94. Available under a CC BY 4.0 DEED License. Copyright 2024 Ananta Dey et al., published by Springer Nature Limited.

(RuCY) grafted onto plasmonic p-GaN/AuNPs via NHCs as linkers instead of conventional thiol linkers for CO_2-to-formate conversion.[92] The photoelectrochemical setup consisting of (p-GaN/AuNP/RuCY) demonstrated a full reaction (Figure 6a). Here, water oxidation occurred at the anode in tandem with reduction of CO_2 to formate at the cathode. The NHC-RuCY covalent linkage could lessen the overpotential and surface resistance for efficient hot electron transfer at a lower overpotential than bare p-GaN/AuNPs (Figure 6b). This unique functionalization ensured selectivity for formate as the desired product instead of CO, with a FE of 96.8%. Thus, there is ample room for improvement in molecular catalyst and plasmonic nanoparticle heterojunction design, and a pool of easily tunable hybrid systems can be developed for better reactivity and selectivity.

In addition to energy transfer, nanoparticles can offer stability and structural support to the molecular catalyst, shielding it from degradation. In a recent study, Baumberg and co-workers utilized a plasmonic gap approach to create a hybrid structure where a nickel bis(terpyridine) complex $[Ni(tpyS)_2]$ is sandwiched between two gold surfaces forming a nanogap (Figure 7a).[93] Dark-field spectral studies were utilized to characterize the monolayer quality in the gap. The molecular complex exhibits high selectivity for CO_2RR toward CO production over hydrogen in the solution phase catalysis. The reaction mechanism changes in the hybrid catalyst

https://doi.org/10.1021/acsnanoscienceau.4c00009
ACS Nanosci. Au 2024, 4, 273−289

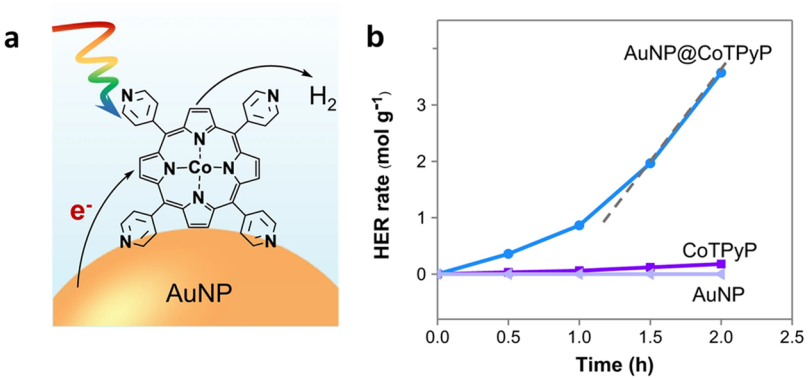

Figure 9. (a) Schematic illustration of AuNP@CoTPyP nanohybrids. (b) Photocatalytic HER curves of AuNP, CoTPyP, and AuNP@CoTPyP. Reproduced from ref 100. Available under a CC BY 4.0 DEED License. Copyright 2023 Huixiang Sheng et al., published by Springer Nature Limited.

compared with the original molecular catalyst as the electron transferred during reduction delocalizes over the Au−S anchoring unit and protects the integrity of the molecular framework by inhibiting any ligand loss (Figure 7c). The comparison of experimental surface-enhanced Raman scattering (SERS) spectra with the density functional theory (DFT) calculated spectra displays the weakening of the Au−S bond while no discernible changes in the active center environment were observed. Thus, the nature of the anchoring unit plays a pivotal role in the selection of the catalytic mechanism. Comparison of the cyclic voltammetry (CV) data of the molecular complex in the presence and absence of AuNPs shows that the catalytic reduction is more favorable in the Au−$Ni(tpyS)_2$ monolayer due to stabilization of reduced radical species. The increased current density and reduced onset potential of the Au substrate under a CO_2 environment in the presence of a molecular catalyst indicate the occurrence of effective CO_2 reduction (CO_2RR). The nanoparticle stabilizes the molecular species by withdrawing electron density from the monolayer, making reduction easier. SERS-coupled electrochemistry was recorded for both the reduced ($[Ni(tpyS)_2]^{+1}$, −0.6 V vs Ag/AgCl), and oxidized ($[Ni(tpyS)_2]^{+2}$, 0 V vs Ag/AgCl) states to understand the changes in the chemical bonding of the molecular complex. The resultant spectra illustrate the emergence of several new bands along with an enhancement in the SERS background during reduction. The experimental spectra show best agreement with the calculated SERS when $[Ni(tpyS)_2\text{-}H_2O]^{+2}$ is considered as the reduced species (Figure 7b). Additionally, the solution-state reduction of the non-thiolated catalyst suggests the loss of one terpyridine ligand, which is avoided in the unique sandwiched structure of the hybrid. In accordance with the experimental SERS results and DFT measurements, the authors proposed a $2H^+/2e^-$ reduction pathway and explored possible intermediates (Figure 7c).

Recently, Sá and co-workers reported a plasmonic nanohybrid system NiO/Au/Re^I(phen-NH_2)$(CO)_3Cl$ (phen-NH_2 = 1,10-phenanthrolin-5-amine) that is unstable above 580 K to limit the plasmon thermal contribution, ensuring that hot carriers are the primary contributors to the catalytic process[94] (Figure 8). The experiment utilized a nanohybrid comprising a NiO semiconductor as the hole accepting unit and plasmonic AuNPs for hot electron exploitation that is functionalized with an intricately designed Re catalyst for selective CO_2 to CO conversion. The study combines photoelectrocatalysis with advanced in situ spectroscopies, such as transient absorption spectroscopy (TAS), transient infrared absorption spectroscopy (TIRAS), and unbiased in situ FTIR studies, to establish charge transfer dynamics and confirm the direct involvement of hot carriers in the catalytic CO_2RR at room temperature. LSPR photoexcitation of AuNPs results in energetic hot carriers, hot electrons and holes, where hot electrons are injected into the Re catalyst to initiate CO_2 reduction and the hot holes are then injected into NiO to drive the oxygen evolution reaction on the anode. The initial electron transfer to the Re catalyst triggers the reduction of ligands as supported by TIRAS studies and subsequently undergoes two sequential protonations with the second protonation being the rate-limiting step that leads to the release of a water molecule. In the last stage, the second plasmon hot electron reduces Re^I−CO to release CO, thereby concluding the cycle. These findings make a significant contribution to the continuous investigation of plasmonic photocatalysis and offer valuable perspectives on the direct utilization of hot carriers in catalytic processes.

PLASMONIC METAL−MOLECULAR COMPLEXES FOR H_2 GENERATION

Photocatalytic hydrogen production is an important method for the conversion of solar energy into chemical energy, providing a pathway to produce clean and renewable energy for a green future.[95] However, the implementation of a hydrogen-energy-based economy at an industrial scale remains challenging due to the difficulties associated with the development of reliable H_2 storage/delivery systems. The two major categories of sources for photocatalytic hydrogen production are as follows: (a) *Water:* The hydrogen evolution reaction (HER) using water and solar power is an efficient and environment-friendly method due to the abundance of both water and sunlight. (b) *Other hydrogen-containing compounds*: Compounds with a high hydrogen content like formic acid (HCOOH),[96] ammonia borane (NH_3BH_3),[97,98] or sodium borohydride ($NaBH_4$) are gaining traction, especially for their ease of transport and storage. To date, inorganic semiconductors and organic molecules are widely utilized as catalysts for photocatalytic HER. The molecular complexes have the advantage of easy modulation and tunability of their fundamental properties.[28] However, molecular complexes often suffer from poor light-absorbing ability and low photostability, hampering the catalytic rate.[99] In recent years, there has been growing interest in utilizing molecular catalysts

https://doi.org/10.1021/acsnanoscienceau.4c00009
ACS Nanosci. Au 2024, 4, 273−289

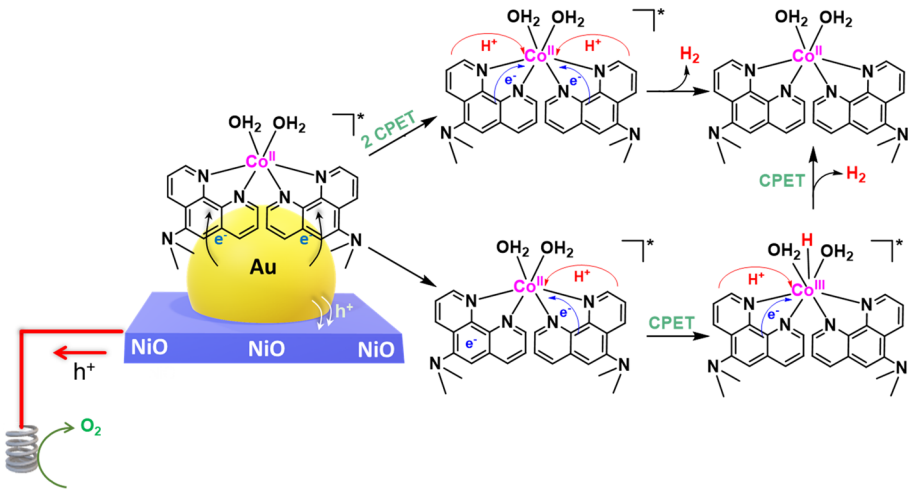

Figure 10. Schematic representation of the catalytic cycle leading to H_2 evolution with a NiO/Au/[Co(1,10-phenanthrolin-5-amine)$_2$(H_2O)$_2$] plasmonic nanohybrid system. Recreated from ref 101. Available under a CC BY 4.0 DEED License. Copyright 2024, Ananta Dey et al., published by Springer Nature Limited.

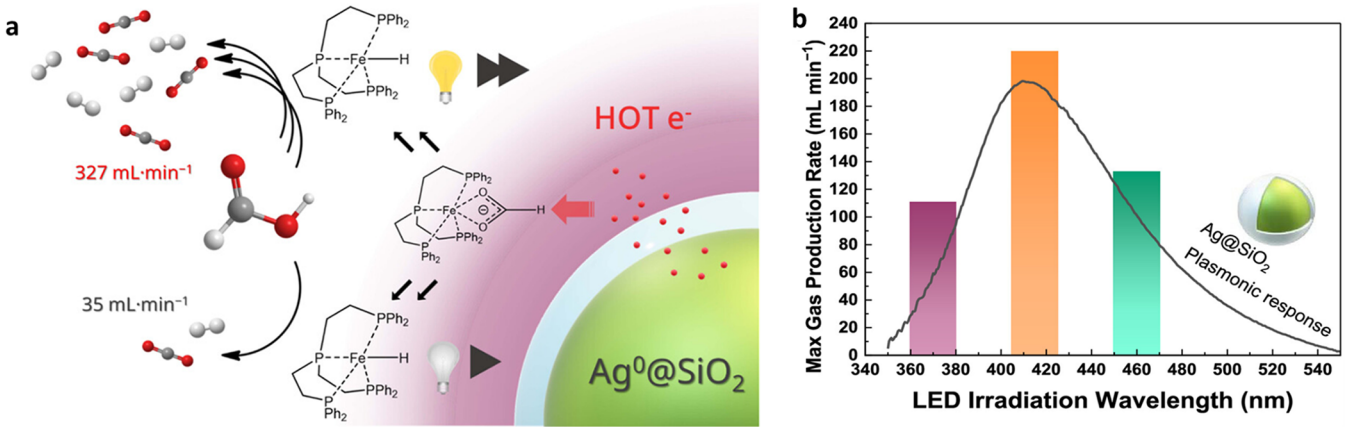

Figure 11. (a) Schematic illustration of the involvement of hot electrons in the catalytic cycle of the [Ag^0@SiO_2/(Fe/PP_3)/HCOOH] system. (b) Gas production rate enhancement for the three LED light sources (purple: LED-365, orange: LED-405, green: LED-455). Adapted with permission from ref 102. Copyright 2023 American Chemical Society.

in combination with plasmonic materials for efficient hydrogen production. In this section, we will explore some of the recent advances made in this field.

Lu et al. developed a highly efficient and stable photocatalytic system comprising a molecular catalyst of cobalt porphyrin with plasmonic gold nanoparticles for the hydrogen evolution reaction (HER) (Figure 9a).[100] The synergy between the two constituents (AuNPs and CoTPyP molecules) enhanced the charge separation and its subsequent transfer at the interface, leading to a remarkable enhancement in the catalytic HER performance. The AuNPs are chemically inert for HER reactions when used alone, and CoTPyP alone exhibits a low HER rate of 0.09 mol g^{-1} h^{-1} (Figure 9b). However, when combined, AuNP@CoTPyP showed strong catalytic activity toward HER (Figure 9b). The hybrid catalyst exhibits long-term stability up to 45 h of continuous photocatalytic reaction. The plasmonic effects, specifically LSPR and interface charge transfer, play pivotal roles in augmenting the photocatalytic activity of the AuNP@CoTPyP nanostructures. A higher concentration of CoTPyP molecules affects the catalytic activity due to the decreased aggregation of AuNPs, which further reduces the formation of gap-mode plasmonic hotspots essential for photocatalytic HER activity. In contrast to that with spherical AuNPs, the HER on gold nanorods exhibited a marginally lower rate of 0.2 mol g^{-1} h^{-1} due to the smaller gap-mode plasmonic hotspots generated in the nanorods. Supplementary studies revealed that the transfer of hot carriers to the CoTPyP molecules led to inhibition of the radiative decay pathway, resulting in an increased HER rate. Finally, DFT calculations support the experimental observations of enhanced charge transfer and catalytic activity in the AuNP@CoTPyP system, providing critical insights into the mechanism underlying the photocatalytic HER process.

Recently, Sá et al. directly utilized plasmonic hot electrons generated with visible light irradiation for catalytic HER.[101] Here, the focus was to distinguish between photothermal and hot-carrier mechanisms in plasmonic-driven catalysis. To ensure that the hot carriers can act as the major contributors to the catalytic process, the plasmonic nanohybrid system NiO/Au/[Co(1,10-phenanthrolin-5-amine)$_2$(H_2O)$_2$] was deliberately assembled to limit the plasmon thermal contribution. The authors demonstrated the role of plasmonic hot electrons, which enhanced the hydrogen evolution rate when directed into phenanthroline ligands, as the characteristic features of a hot-carrier-mediated process were consistent with the catalytic response to light modulation. In the catalytic mechanism, the

https://doi.org/10.1021/acsnanoscienceau.4c00009
ACS Nanosci. Au 2024, 4, 273−289

Table 1. Plasmonic Metal−Molecular Complex Hybrids for Various Catalytic Processes

plasmonic material	molecular catalyst	light source	reaction	major product (% selectivity)	temp	performance metrics[a]	stability (h)	PE[b]	ref
ZIS-Au/Ag NP	FeTCPP	300 W Xe lamp >420 nm	CO_2RR	CO			9		63
Au/TiO_2	RuCY	300 or 450 W Xe lamp	CO_2RR	HCOOH (95%)		TOF = 1200 h^{-1}	50		67
Ag/TaON	RuBLRu′	500 W Hg lamp >400 nm	CO_2RR	HCOOH (60%)		Φ = 0.20, TOF = 5 h^{-1}, TON = 41	24	14	68
Ag/TaON	RuRu′	500 W Hg lamp >400 nm	CO_2RR	HCOOH (85%)	298 ± 2 K	Φ = 0.0023, TOF = 25 h^{-1}, TON = 620	24	6	69
Ag/C_3N_4	RuRu′	400 W Hg lamp >400 nm	CO_2RR	HCOOH (99%)	rt	Φ = 0.052, TON = 33000	48	70	70
Ag/C_3N_4	RuRu′	Xe lamp >400 nm	CO_2RR	HCOOH (98%)		Φ = 0.2, TOF = 139 h^{-1}, TON = 2090	15		72
Ag/C_3N_4	RuP	400 W Hg lamp >400 nm	CO_2RR	HCOOH (95%)	473 K	Φ = 4.2, TON = 5775	96		71
Ag/C_3N_4	RuCP	LED (400 nm)	CO_2RR	HCOOH (95%)		Φ = 1.4, TOF = 800 h^{-1}, TON = 12000	60	44	73
Ag nanocubes	$[ReTC]_3$-MOF	300 W Xe lamp (400−700 nm)	CO_2RR	CO (96%)		TOF = 1.4 × 10^{-2} h^{-1}	48	7	87
p-GaN/ AuNPs	RuCY	Xe lamp >400 nm	CO_2RR	HCOOH (96.8%)		TOF = 1.46 min^{-1}, TO N = 1757	20		92
AuNP	$Ni(tpyS)_2$		CO_2RR	CO					93
AuNP	$Re^{I}(phen\text{-}NH_2)(CO)_3Cl$	532 nm laser	CO_2RR	CO	295 K	TOF = 0.156 min^{-1}, Φ = 0.2%	3		94
AuNP	CoTPyP	300 W Xe lamp >400 nm	HER	H_2	50 °C	R = 3.21 mol g^{-1} h^{-1}, 4650 h^{-1}	45	20.8	100
AuNP	[Co(1,10-phenanthrolin-5-amine)$_2$(H_2O)$_2$]	CW laser 532 nm	HER	H_2	265 °C				101
Ag@SiO_2	Fe/PP_3	300 W Xe lamp, LED	H_2 production (FADH)	H_2/CO_2 (1:1)	80 °C	TON = 35643, TOF = 17821 h^{-1}		10	102
Au(111)	FePc		ORR	H_2O_2					103
Au(111)	CoPc		ORR	H_2O_2					104
AuTNP	cobaloxime	white light supercontinuum laser	WOR	O_2, H_2		Φ = 0.8, R_{H_2} = 1.32 μmol h^{-1}, R_{O_2} = 0.66 μmol h^{-1}			27

[a]Performance of catalyst calculated only for major product in terms of TOF, TON, formation rate (R), and quantum yield (Φ). [b]Plasmonic enhancement (PE)= the ratio of the overpotential shift for an electrocatalyst under illuminated conditions in the presence and absence of the plasmonic component. As PE is a ratio, it is unitless.

irradiated AuNPs generate hot electrons and holes. The hot holes transfer to NiO, leading to O_2 production at the counter electrode. The hot electrons are transferred to the phen ligand and delocalize in the aromatic ring. These electrons further undergo CPET (concerted proton−electron transfer) via either a simultaneous or a sequential pathway, leading to H_2 production (Figure 10). Thus, this work sheds light on the complex processes of thermal contribution and charge transfer from plasmonic AuNPs, emphasizing how crucial it is to comprehend ultrafast charge dynamics in plasmon mediated photoelectrochemical catalytic systems. This investigation definitively settles the enduring dispute concerning the direct participation of hot electrons in plasmon−molecular complex hybrid photoreactor assemblies.

Gemenetzi et al. demonstrated photoplasmon-mediated formic acid dehydrogenation (FADH) to increase H_2 production.[102] The photoexcited core−shell Ag^0@SiO_2 plasmonic nanoparticles (PNPs) and a molecular Fe catalyst amplified hydrogen production by ∼4-fold (TON = 35,643) compared to the experiment where the catalyst was used alone (TON = 9615). Hydrogen production is dependent on the catalytic activation of formic acid, which produces a transient intermediate called Fe-hydride (Figure 11a). The mechanism involved in this process entails a decrease in the solution potential (E_h) triggered by the production of reducing agents in the reaction solution by Ag^0@SiO_2 PNPs. Through selective excitation at wavelengths (λ_{ex}) ranging over the photoactive profile of the nanohybrid, maximum FADH response was observed at λ_{ex} = 405 nm (Figure 11b). Hence, these reducing agents help to enhance the rates of H_2 production. The FADH reaction rate was further amplified by controlling the hot electron injection rates by varying the SiO_2 shell thickness, which ranged between 3 and 5 nm. Thus, this work expands the possibilities for producing hydrogen on an industrial scale by using FADH.

PLASMONIC METAL−MOLECULAR COMPLEXES FOR O_2 EVOLUTION/REDUCTION

Aside from the CO_2RR and HER, many ongoing studies on plasmon-assisted molecular catalysis also include oxygen reduction and oxygen evolution reactions (ORR and OER), which are crucial for the development of fuel cells. Wan et al. investigated a highly ordered iron phthalocyanine (FePc) adlayer on Au(111) electrode for ORR.[103] From CV results, it was clear that FePc-modified Au(111) shows significantly higher catalytic activity than the bare Au electrode. Similarly, Van Duyne et al. utilized a cobalt phthalocyanine (CoPc) modified Au(111) substrate for ORR.[104] Previously, they also

https://doi.org/10.1021/acsnanoscienceau.4c00009
ACS Nanosci. Au 2024, 4, 273−289

employed the CoPc/Ag(111) system and observed strong evidence for oxygen activation due to the chemisorption of O_2 on well-ordered CoPc monolayers supported on the Ag(111) surface.[105] These studies are limited to analysis of electrochemical catalytic activity yet quite insightful in presenting strategies for anchoring of molecular complexes on Au/Ag(111) electrode surfaces and outline *in situ* spectroscopic studies such as *in situ* electrochemical scanning tunneling microscopy (EC-STM), electrochemical tip-enhanced Raman spectroscopy (EC-TERS), etc. to probe molecular scale catalytic interactions. Recently, our group[27] has utilized a cobaloxime complex covalently linked with Au triangular nanoprisms for efficient photoelectrocatalytic water oxidation reaction (WOR/OER). The gold plasmon−cobalt catalyst dyad retains its stability and integrity during the catalytic reaction and successfully imitates photosystem II for neutral water oxidation in the visible−NIR region of the solar spectrum. Therefore, there is a substantial gap to address and numerous opportunities to explore plasmon-induced molecular oxygen evolution reaction (OER) and oxygen reduction reaction (ORR) using comprehensive plasmon−molecular complex dyads across the entire solar spectrum.

OUTLOOK AND CONCLUSION

In this review, we have pursued deeper insight into the untapped potential of hybrids of plasmonic noble metal nanoparticles and synthetic molecular catalysts leading to a range of small molecule activation reactions. Incorporating plasmonic nanomaterials with molecular complexes has opened a new avenue to explore highly reactive and selective artificial photosynthetic catalytic models. The surface plasmon resonance phenomenon in noble metal nanoparticles allows the harvesting of photons from visible to near-infrared spectral regions by explicitly manipulating the shapes and dimensions of nanoparticles. Noble metal nanoparticles, thus acting as efficient antennas for light energy, generate energetic charge carriers that can be harnessed to drive chemical reactions with enhanced catalytic rate and selectivity and lowered energy requirements. Their ultrafast charge transfer dynamics down to a time scale of femtoseconds, however, pose difficulties in their direct utilization as photocatalysts. Thus, plasmonic metal nanohybrids with different catalytic units have been explored in an efficient strategy to achieve optimum charge separation and transfer to an adsorbate molecule for its activation. The benefits of molecular catalysts have been widely acknowledged in homogeneous catalytic conditions, as they allow for fine-tuning the reactive metal centers and easy modulation of steric and electronic features by introducing different functionalities. Such molecular catalytic platforms offer a broad avenue for gaining insights into the reaction mechanisms and intermediate species formed, as revealed by mechanistic and spectroscopic investigations. Thus, integrating the best of two worlds, plasmonic nanoparticles for their excellent optical properties and molecular catalysts for well-defined molecular structure and active metal center, a wealth of prospects emerge in the realm of catalysis.

Herein, we have briefly discussed the fundamental photophysical properties and plasmon-mediated interfacial charge transfer pathways. Further, we have established a juxtaposition among noble and earth-abundant plasmonic metals based on their spectral absorption profiles, stability, and the convenience of their synthesis and functionalization. After laying the foundations of plasmonic effects, we have concisely reviewed the plasmon−molecular catalyst photocathodes, as summarized in Table 1, reported for CO_2 reduction, hydrogen evolution reaction, and oxygen evolution/reduction. The high cost of precious-metal-based nanoparticles has often been cited as a limitation of their large-scale production in the commercial sector. However, the strong light−matter interactions occurring in the full solar spectrum (visible to NIR) and near-field enhancement on the order of 10^3 in hotspot regions in proximity to the plasmon cannot be overlooked while proving their mettle as robust light harvesters. In addition, grafting molecular catalysts to plasmon-based solid photocathodes broadens the scope of utilization of metal complexes in heterogeneous conditions exhibiting synergistic amelioration in catalytic activity, improved stability, and reusability. There exists a vast potential in exploring earth-abundant plasmonic nanoparticle and molecular catalyst hybrids to mediate catalytic transformations such as nitrate reduction, ammonia oxidation, nitrogen reduction, oxygen reduction reaction, etc. Molecular catalysts integrated with PNPs can be used to understand the underlying plasmon-induced hot carrier generation/injection or photothermal reaction mechanistic pathways involved in plasmonic enhancement in chemical conversion through ultrafast transient absorption spectroscopic studies. Therefore, the plasmonic−molecular complex hybrids showcase the potential of an ideal photocatalytic core that can set up the template for sustainable and scalable solar-energy-driven energy-relevant small molecule transformation reactions.

AUTHOR INFORMATION

Corresponding Author

Arnab Dutta − *Interdisciplinary Program Climate Studies, Indian Institute of Technology Bombay, Mumbai, Maharashtra 400076, India; Chemistry Department, Indian Institute of Technology Bombay, Mumbai, Maharashtra 400076, India; National Centre of Excellence in Carbon Capture and Utilization, Mumbai, Maharashtra 400076, India;* orcid.org/0000-0002-9998-6329; Email: arnab.dutta@iitb.ac.in

Authors

Tannu Kaushik − *Interdisciplinary Program Climate Studies, Indian Institute of Technology Bombay, Mumbai, Maharashtra 400076, India*

Suchismita Ghosh − *Chemistry Department, Indian Institute of Technology Bombay, Mumbai, Maharashtra 400076, India*

Thinles Dolkar − *Chemistry Department, Indian Institute of Technology Bombay, Mumbai, Maharashtra 400076, India*

Rathindranath Biswas − *Chemistry Department, Indian Institute of Technology Bombay, Mumbai, Maharashtra 400076, India;* orcid.org/0000-0002-0909-1442

Complete contact information is available at: https://pubs.acs.org/10.1021/acsnanoscienceau.4c00009

Author Contributions

[▽]T.K. and S.G. have contributed equally. CRediT: **Tannu Kaushik** conceptualization, writing-original draft, writing-review & editing; **Suchismita Ghosh** conceptualization, writing-original draft, writing-review & editing; **Thinles Dolkar** writing-review & editing; **Rathindranath Biswas** writing-review & editing; **Arnab Dutta** conceptualization,

https://doi.org/10.1021/acsnanoscienceau.4c00009
ACS Nanosci. Au 2024, 4, 273−289

project administration, supervision, writing-original draft, writing-review & editing.

Notes

The authors declare no competing financial interest.

■ ACKNOWLEDGMENTS

The authors thank DST, India-supported National Center of Excellence (DST/TMD/CCUS/CoE/202/IITB), for the support for this research activity. T.K. thanks PMRF fellowship (PMRF ID:1302078) for financial support.

■ REFERENCES

(1) Friedlingstein, P.; O'Sullivan, M.; Jones, M. W.; Andrew, R. M.; Bakker, D. C. E.; Hauck, J.; Landschützer, P.; Le Quéré, C.; Luijkx, I. T.; Peters, G. P.; Peters, W.; Pongratz, J.; Schwingshackl, C.; Sitch, S.; Canadell, J. G.; Ciais, P.; Jackson, R. B.; Alin, S. R.; Anthoni, P.; Barbero, L.; Bates, N. R.; Becker, M.; Bellouin, N.; Decharme, B.; Bopp, L.; Brasika, I. B. M.; Cadule, P.; Chamberlain, M. A.; Chandra, N.; Chau, T.-T.-T.; Chevallier, F.; Chini, L. P.; Cronin, M.; Dou, X.; Enyo, K.; Evans, W.; Falk, S.; Feely, R. A.; Feng, L.; Ford, D. J.; Gasser, T.; Ghattas, J.; Gkritzalis, T.; Grassi, G.; Gregor, L.; Gruber, N.; Gürses, Ö.; Harris, I.; Hefner, M.; Heinke, J.; Houghton, R. A.; Hurtt, G. C.; Iida, Y.; Ilyina, T.; Jacobson, A. R.; Jain, A.; Jarníková, T.; Jersild, A.; Jiang, F.; Jin, Z.; Joos, F.; Kato, E.; Keeling, R. F.; Kennedy, D.; Klein Goldewijk, K.; Knauer, J.; Korsbakken, J. I.; Körtzinger, A.; Lan, X.; Lefèvre, N.; Li, H.; Liu, J.; Liu, Z.; Ma, L.; Marland, G.; Mayot, N.; McGuire, P. C.; McKinley, G. A.; Meyer, G.; Morgan, E. J.; Munro, D. R.; Nakaoka, S.-I.; Niwa, Y.; O'Brien, K. M.; Olsen, A.; Omar, A. M.; Ono, T.; Paulsen, M.; Pierrot, D.; Pocock, K.; Poulter, B.; Powis, C. M.; Rehder, G.; Resplandy, L.; Robertson, E.; Rödenbeck, C.; Rosan, T. M.; Schwinger, J.; Séférian, R.; Smallman, T. L.; Smith, S. M.; Sospedra-Alfonso, R.; Sun, Q.; Sutton, A. J.; Sweeney, C.; Takao, S.; Tans, P. P.; Tian, H.; Tilbrook, B.; Tsujino, H.; Tubiello, F.; Van Der Werf, G. R.; Van Ooijen, E.; Wanninkhof, R.; Watanabe, M.; Wimart-Rousseau, C.; Yang, D.; Yang, X.; Yuan, W.; Yue, X.; Zaehle, S.; Zeng, J.; Zheng, B. Global Carbon Budget 2023. *Earth Syst. Sci. Data* **2023**, *15* (12), 5301−5369.

(2) Lewis, N. S. Toward Cost-Effective Solar Energy Use. *Science* **2007**, *315* (5813), 798−801.

(3) Lewis, N. S.; Nocera, D. G. Powering the Planet: Chemical Challenges in Solar Energy Utilization. *Proc. Natl. Acad. Sci. U.S.A.* **2006**, *103* (43), 15729−15735.

(4) Maugh, T. H. Catalysis in Solar Energy: Photoelectrochemical Cells Approach the Efficiency of Photovoltaics, but Durability and Cost Are Still Major Hurdles. *Science* **1983**, *221* (4618), 1358−1361.

(5) MacDowell, N.; Florin, N.; Buchard, A.; Hallett, J.; Galindo, A.; Jackson, G.; Adjiman, C. S.; Williams, C. K.; Shah, N.; Fennell, P. An Overview of CO2 Capture Technologies. *Energy Environ. Sci.* **2010**, *3* (11), 1645.

(6) Nichols, E. M.; Gallagher, J. J.; Liu, C.; Su, Y.; Resasco, J.; Yu, Y.; Sun, Y.; Yang, P.; Chang, M. C. Y.; Chang, C. J. Hybrid Bioinorganic Approach to Solar-to-Chemical Conversion. *Proc. Natl. Acad. Sci. U.S.A.* **2015**, *112* (37), 11461−11466.

(7) Shevela, D.; Björn, L. O.; Govindjee *Photosynthesis: Solar Energy for Life*; WORLD SCIENTIFIC, 2018; DOI: 10.1142/10522.

(8) Shen, L.; Yin, X. Solar Spectral Management for Natural Photosynthesis: From Photonics Designs to Potential Applications. *Nano Convergence* **2022**, *9* (1), 36.

(9) Takakura, R.; Oshikiri, T.; Ueno, K.; Shi, X.; Kondo, T.; Masuda, H.; Misawa, H. Water Splitting Using a Three-Dimensional Plasmonic Photoanode with Titanium Dioxide Nano-Tunnels. *Green Chem.* **2017**, *19* (10), 2398−2405.

(10) Rahaman, M.; Andrei, V.; Wright, D.; Lam, E.; Pornrungroj, C.; Bhattacharjee, S.; Pichler, C. M.; Greer, H. F.; Baumberg, J. J.; Reisner, E. Solar-Driven Liquid Multi-Carbon Fuel Production Using a Standalone Perovskite-BiVO4 Artificial Leaf. *Nat. Energy* **2023**, *8* (6), 629−638.

(11) Aziz, S. K. T.; Banerjee, A.; Kaushik, T.; Saha, S.; Dutta, A. Exploring the Hydrogen Evolution Reaction (HER) Side of Perovskite-Based Materials during Photoelectrochemical Water Splitting. In *Solar-Driven Green Hydrogen Generation and Storage*; Elsevier, 2023; pp 1−21, DOI: 10.1016/B978-0-323-99580-1.00010-8.

(12) Moinel, A.; Brochnow, M.; Aumaître, C.; Giannoudis, E.; Fize, J.; Saint-Pierre, C.; Pécaut, J.; Maldivi, P.; Artero, V.; Demadrille, R.; Chavarot-Kerlidou, M. Push-Pull Organic Dyes and Dye-Catalyst Assembly Featuring a Benzothiadiazole Unit for Photoelectrochemical Hydrogen Production. *Sustainable Energy Fuels* **2022**, *6* (15), 3565−3572.

(13) Kim, J.; Son, H. Y.; Nam, Y. S. Multilayered Plasmonic Heterostructure of Gold and Titania Nanoparticles for Solar Fuel Production. *Sci. Rep* **2018**, *8* (1), 10464.

(14) Joshi, G.; Mir, A. Q.; Layek, A.; Ali, A.; Aziz, Sk. T.; Khatua, S.; Dutta, A. Plasmon-Based Small-Molecule Activation: A New Dawn in the Field of Solar-Driven Chemical Transformation. *ACS Catal.* **2022**, *12* (2), 1052−1067.

(15) Ji, Z.; He, M.; Huang, Z.; Ozkan, U.; Wu, Y. Photostable P-Type Dye-Sensitized Photoelectrochemical Cells for Water Reduction. *J. Am. Chem. Soc.* **2013**, *135* (32), 11696−11699.

(16) Ma, Y.; Wang, X.; Jia, Y.; Chen, X.; Han, H.; Li, C. Titanium Dioxide-Based Nanomaterials for Photocatalytic Fuel Generations. *Chem. Rev.* **2014**, *114* (19), 9987−10043.

(17) Tran, P. D.; Wong, L. H.; Barber, J.; Loo, J. S. C. Recent Advances in Hybrid Photocatalysts for Solar Fuel Production. *Energy Environ. Sci.* **2012**, *5* (3), 5902.

(18) Boutin, E.; Merakeb, L.; Ma, B.; Boudy, B.; Wang, M.; Bonin, J.; Anxolabéhère-Mallart, E.; Robert, M. Molecular Catalysis of CO_2 Reduction: Recent Advances and Perspectives in Electrochemical and Light-Driven Processes with Selected Fe, Ni and Co Aza Macrocyclic and Polypyridine Complexes. *Chem. Soc. Rev.* **2020**, *49* (16), 5772−5809.

(19) Seif-Eddine, M.; Cobb, S. J.; Dang, Y.; Abdiaziz, K.; Bajada, M. A.; Reisner, E.; Roessler, M. M. Operando Film-Electrochemical EPR Spectroscopy Tracks Radical Intermediates in Surface-Immobilized Catalysts. *Nat. Chem.* **2024**, DOI: 10.1038/s41557-024-01450-y.

(20) Nikolaou, V.; Govind, C.; Balanikas, E.; Bharti, J.; Diring, S.; Vauthey, E.; Robert, M.; Odobel, F. Antenna Effect in Noble Metal-Free Dye-Sensitized Photocatalytic Systems Enhances CO_2-to-CO Conversion. *Angew. Chem. Int. Ed* **2024**, *63* (13), No. e202318299.

(21) Shon, J.-H.; Teets, T. S. Photocatalysis with Transition Metal Based Photosensitizers. *Comments on Inorganic Chemistry* **2020**, *40* (2), 53−85.

(22) Liu, X.; Inagaki, S.; Gong, J. Heterogeneous Molecular Systems for Photocatalytic CO_2 Reduction with Water Oxidation. *Angew. Chem. Int. Ed* **2016**, *55* (48), 14924−14950.

(23) Da Silva, A. G. M.; Rodrigues, T. S.; Wang, J.; Camargo, P. H. C. Plasmonic Catalysis with Designer Nanoparticles. *Chem. Commun.* **2022**, *58* (13), 2055−2074.

(24) Wang, H.; Rong, H.; Wang, D.; Li, X.; Zhang, E.; Wan, X.; Bai, B.; Xu, M.; Liu, J.; Liu, J.; Chen, W.; Zhang, J. Highly Selective Photoreduction of CO_2 with Suppressing H_2 Evolution by Plasmonic Au/CdSe-Cu_2O Hierarchical Nanostructures under Visible Light. *Small* **2020**, *16* (18), 2000426.

(25) Guo, F.; Yang, S.; Liu, Y.; Wang, P.; Huang, J.; Sun, W.-Y. Size Engineering of Metal-Organic Framework MIL-101(Cr)-Ag Hybrids for Photocatalytic CO_2 Reduction. *ACS Catal.* **2019**, *9* (9), 8464−8470.

(26) Duflot, M.; Marchal, C.; Caps, V.; Artero, V.; Christoforidis, K.; Keller, V. Optimization of NH2-UiO-66/TiO2/Au Composites for Enhanced Gas-Phase CO2 Photocatalytic Reduction into CH4. *Catal. Today* **2023**, *413*−*415*, 114018.

(27) Mir, A. Q.; Joshi, G.; Ghosh, P.; Khandelwal, S.; Kar, A.; Hegde, R.; Khatua, S.; Dutta, A. Plasmonic Gold Nanoprism-Cobalt Molecular Complex Dyad Mimics Photosystem-II for Visible-NIR Illuminated Neutral Water Oxidation. *ACS Energy Lett.* **2019**, *4* (10), 2428−2435.

(28) Yuan, Y.-J.; Yu, Z.-T.; Chen, D.-Q.; Zou, Z.-G. Metal-Complex Chromophores for Solar Hydrogen Generation. *Chem. Soc. Rev.* **2017**, *46* (3), 603−631.
(29) Rajeshwaree, B.; Ali, A.; Mir, A. Q.; Grover, J.; Lahiri, G. K.; Dutta, A.; Maiti, D. Group 6 Transition Metal-Based Molecular Complexes for Sustainable Catalytic CO $_2$ Activation. *Catal. Sci. Technol.* **2022**, *12* (2), 390−408.
(30) Moularas, C.; Gemenetzi, A.; Deligiannakis, Y.; Louloudi, M. Nanoplasmonics in Catalysis for Energy Technologies: The Concept of Plasmon-Assisted Molecular Catalysis (PAMC). *Nanoenergy Advances* **2024**, *4* (1), 25−44.
(31) Yu, H.; Peng, Y.; Yang, Y.; Li, Z.-Y. Plasmon-Enhanced Light-Matter Interactions and Applications. *npj Comput. Mater.* **2019**, *5* (1), 45.
(32) Kelly, K. L.; Coronado, E.; Zhao, L. L.; Schatz, G. C. The Optical Properties of Metal Nanoparticles: The Influence of Size, Shape, and Dielectric Environment. *J. Phys. Chem. B* **2003**, *107* (3), 668−677.
(33) Clavero, C. Plasmon-Induced Hot-Electron Generation at Nanoparticle/Metal-Oxide Interfaces for Photovoltaic and Photocatalytic Devices. *Nature Photon* **2014**, *8* (2), 95−103.
(34) Yu, S.; Jain, P. K. The Chemical Potential of Plasmonic Excitations. *Angew. Chem. Int. Ed* **2020**, *59* (5), 2085−2088.
(35) Kamarudheen, R.; Aalbers, G. J. W.; Hamans, R. F.; Kamp, L. P. J.; Baldi, A. Distinguishing Among All Possible Activation Mechanisms of a Plasmon-Driven Chemical Reaction. *ACS Energy Lett.* **2020**, *5* (8), 2605−2613.
(36) Ezendam, S.; Herran, M.; Nan, L.; Gruber, C.; Kang, Y.; Gröbmeyer, F.; Lin, R.; Gargiulo, J.; Sousa-Castillo, A.; Cortés, E. Hybrid Plasmonic Nanomaterials for Hydrogen Generation and Carbon Dioxide Reduction. *ACS Energy Lett.* **2022**, *7* (2), 778−815.
(37) Hu, C.; Chen, X.; Low, J.; Yang, Y.-W.; Li, H.; Wu, D.; Chen, S.; Jin, J.; Li, H.; Ju, H.; Wang, C.-H.; Lu, Z.; Long, R.; Song, L.; Xiong, Y. Near-Infrared-Featured Broadband CO2 Reduction with Water to Hydrocarbons by Surface Plasmon. *Nat. Commun.* **2023**, *14* (1), 221.
(38) Paital, D.; Bansal, T.; Kaushik, T.; Joshi, G.; Sett, S.; Khatua, S. Insight into the Photocatalytic and Photothermal Effect in Plasmon-Enhanced Water Oxidation Property of AuTNP@MnOx Core-Shell Nanoconstruct. *J. Chem. Phys.* **2023**, *159* (23), 234703.
(39) Joshi, G.; Saha, A.; Dutta, A.; Khatua, S. NIR-Driven Photocatalytic Hydrogen Production by Silane- and Tertiary Amine-Bound Plasmonic Gold Nanoprisms. *ACS Appl. Mater. Interfaces* **2022**, *14* (34), 38815−38823.
(40) Mukherjee, S.; Libisch, F.; Large, N.; Neumann, O.; Brown, L. V.; Cheng, J.; Lassiter, J. B.; Carter, E. A.; Nordlander, P.; Halas, N. J. Hot Electrons Do the Impossible: Plasmon-Induced Dissociation of H $_2$ on Au. *Nano Lett.* **2013**, *13* (1), 240−247.
(41) Shangguan, W.; Liu, Q.; Wang, Y.; Sun, N.; Liu, Y.; Zhao, R.; Li, Y.; Wang, C.; Zhao, J. Molecular-Level Insight into Photocatalytic CO2 Reduction with H2O over Au Nanoparticles by Interband Transitions. *Nat. Commun.* **2022**, *13* (1), 3894.
(42) Ramakrishnan, S. B.; Mohammadparast, F.; Dadgar, A. P.; Mou, T.; Le, T.; Wang, B.; Jain, P. K.; Andiappan, M. Photoinduced Electron and Energy Transfer Pathways and Photocatalytic Mechanisms in Hybrid Plasmonic Photocatalysis. *Advanced Optical Materials* **2021**, *9* (22), 2101128.
(43) Devasia, D.; Wilson, A. J.; Heo, J.; Mohan, V.; Jain, P. K. A Rich Catalog of C-C Bonded Species Formed in CO2 Reduction on a Plasmonic Photocatalyst. *Nat. Commun.* **2021**, *12* (1), 2612.
(44) Chintawar, C. C.; Yadav, A. K.; Kumar, A.; Sancheti, S. P.; Patil, N. T. Divergent Gold Catalysis: Unlocking Molecular Diversity through Catalyst Control. *Chem. Rev.* **2021**, *121* (14), 8478−8558.
(45) Christopher, P.; Xin, H.; Linic, S. Visible-Light-Enhanced Catalytic Oxidation Reactions on Plasmonic Silver Nanostructures. *Nature Chem.* **2011**, *3* (6), 467−472.
(46) Wu, C.; Zhou, X.; Wei, J. Localized Surface Plasmon Resonance of Silver Nanotriangles Synthesized by a Versatile Solution Reaction. *Nanoscale Res. Lett.* **2015**, *10* (1), 354.
(47) Corson, E. R.; Creel, E. B.; Kostecki, R.; Urban, J. J.; McCloskey, B. D. Effect of Pressure and Temperature on Carbon Dioxide Reduction at a Plasmonically Active Silver Cathode. *Electrochim. Acta* **2021**, *374*, 137820.
(48) Alcorn, F. M.; Van Der Veen, R. M.; Jain, P. K. In Situ Electron Microscopy of Transformations of Copper Nanoparticles under Plasmonic Excitation. *Nano Lett.* **2023**, *23* (14), 6520−6527.
(49) Gawande, M. B.; Goswami, A.; Felpin, F.-X.; Asefa, T.; Huang, X.; Silva, R.; Zou, X.; Zboril, R.; Varma, R. S. Cu and Cu-Based Nanoparticles: Synthesis and Applications in Catalysis. *Chem. Rev.* **2016**, *116* (6), 3722−3811.
(50) Zhang, Y.; Cai, B.; Jia, B. Ultraviolet Plasmonic Aluminium Nanoparticles for Highly Efficient Light Incoupling on Silicon Solar Cells. *Nanomaterials* **2016**, *6* (6), 95.
(51) Costentin, C.; Robert, M.; Savéant, J.-M.; Tatin, A. Efficient and Selective Molecular Catalyst for the CO $_2$ -to-CO Electrochemical Conversion in Water. *Proc. Natl. Acad. Sci. U.S.A.* **2015**, *112* (22), 6882−6886.
(52) Schneider, J.; Jia, H.; Muckerman, J. T.; Fujita, E. Thermodynamics and Kinetics of CO2, CO, and H+ Binding to the Metal Centre of CO2reductioncatalysts. *Chem. Soc. Rev.* **2012**, *41* (6), 2036−2051.
(53) Jeoung, J.-H.; Dobbek, H. Carbon Dioxide Activation at the Ni,Fe-Cluster of Anaerobic Carbon Monoxide Dehydrogenase. *Science* **2007**, *318* (5855), 1461−1464.
(54) Shafaat, H. S.; Yang, J. Y. Uniting Biological and Chemical Strategies for Selective CO2 Reduction. *Nat. Catal* **2021**, *4* (11), 928−933.
(55) Guria, S.; Dolui, D.; Das, C.; Ghorai, S.; Vishal, V.; Maiti, D.; Lahiri, G. K.; Dutta, A. Energy-Efficient CO2/CO Interconversion by Homogeneous Copper-Based Molecular Catalysts. *Nat. Commun.* **2023**, *14* (1), 6859.
(56) Berardi, S.; Drouet, S.; Francàs, L.; Gimbert-Suriñach, C.; Guttentag, M.; Richmond, C.; Stoll, T.; Llobet, A. Molecular Artificial Photosynthesis. *Chem. Soc. Rev.* **2014**, *43* (22), 7501−7519.
(57) Fourmond, V.; Wiedner, E. S.; Shaw, W. J.; Léger, C. Understanding and Design of Bidirectional and Reversible Catalysts of Multielectron, Multistep Reactions. *J. Am. Chem. Soc.* **2019**, *141* (28), 11269−11285.
(58) Yu, S.; Wilson, A. J.; Heo, J.; Jain, P. K. Plasmonic Control of Multi-Electron Transfer and C-C Coupling in Visible-Light-Driven CO $_2$ Reduction on Au Nanoparticles. *Nano Lett.* **2018**, *18* (4), 2189−2194.
(59) Wen, F.; Li, C. Hybrid Artificial Photosynthetic Systems Comprising Semiconductors as Light Harvesters and Biomimetic Complexes as Molecular Cocatalysts. *Acc. Chem. Res.* **2013**, *46* (11), 2355−2364.
(60) Maeda, K. Metal-Complex/Semiconductor Hybrid Photocatalysts and Photoelectrodes for CO $_2$ Reduction Driven by Visible Light. *Adv. Mater.* **2019**, *31* (25), 1808205.
(61) Gao, C.; Wang, J.; Xu, H.; Xiong, Y. Coordination Chemistry in the Design of Heterogeneous Photocatalysts. *Chem. Soc. Rev.* **2017**, *46* (10), 2799−2823.
(62) Garcia-Osorio, D. A.; Shalvey, T. P.; Banerji, L.; Saeed, K.; Neri, G.; Phillips, L. J.; Hutter, O. S.; Casadevall, C.; Antón-García, D.; Reisner, E.; Major, J. D.; Cowan, A. J. Hybrid Photocathode Based on a Ni Molecular Catalyst and Sb_2Se_3 for Solar H_2 Production. *Chem. Commun.* **2023**, *59* (7), 944−947.
(63) Li, P.; Jia, X.; Zhang, J.; Li, J.; Zhang, J.; Wang, L.; Wang, J.; Zhou, Q.; Wei, W.; Zhao, X.; Wang, S.; Sun, H. The Roles of Gold and Silver Nanoparticles on ZnIn2S4/Silver (Gold)/Tetra(4-Carboxyphenyl)Porphyrin Iron(III) Chloride Hybrids in Carbon Dioxide Photoreduction. *J. Colloid Interface Sci.* **2022**, *628*, 831−839.
(64) Bian, Z.; Tachikawa, T.; Zhang, P.; Fujitsuka, M.; Majima, T. Au/TiO $_2$ Superstructure-Based Plasmonic Photocatalysts Exhibiting Efficient Charge Separation and Unprecedented Activity. *J. Am. Chem. Soc.* **2014**, *136* (1), 458−465.

https://doi.org/10.1021/acsnanoscienceau.4c00009
ACS Nanosci. Au 2024, 4, 273−289

(65) Dodekatos, G.; Tüysüz, H. Plasmonic Au/TiO $_2$ Nanostructures for Glycerol Oxidation. *Catal. Sci. Technol.* **2016**, *6* (19), 7307−7315.
(66) Wang, H.; You, T.; Shi, W.; Li, J.; Guo, L. Au/TiO $_2$ /Au as a Plasmonic Coupling Photocatalyst. *J. Phys. Chem. C* **2012**, *116* (10), 6490−6494.
(67) Jun, H.; Choi, S.; Yang, M. Y.; Nam, Y. S. A Ruthenium-Based Plasmonic Hybrid Photocatalyst for Aqueous Carbon Dioxide Conversion with a High Reaction Rate and Selectivity. *J. Mater. Chem. A* **2019**, *7* (29), 17254−17260.
(68) Sekizawa, K.; Maeda, K.; Domen, K.; Koike, K.; Ishitani, O. Artificial Z-Scheme Constructed with a Supramolecular Metal Complex and Semiconductor for the Photocatalytic Reduction of CO $_2$. *J. Am. Chem. Soc.* **2013**, *135* (12), 4596−4599.
(69) Nakada, A.; Nakashima, T.; Sekizawa, K.; Maeda, K.; Ishitani, O. Visible-Light-Driven CO $_2$ Reduction on a Hybrid Photocatalyst Consisting of a Ru(II) Binuclear Complex and a Ag-Loaded TaON in Aqueous Solutions. *Chem. Sci.* **2016**, *7* (7), 4364−4371.
(70) Kuriki, R.; Matsunaga, H.; Nakashima, T.; Wada, K.; Yamakata, A.; Ishitani, O.; Maeda, K. Nature-Inspired, Highly Durable CO $_2$ Reduction System Consisting of a Binuclear Ruthenium(II) Complex and an Organic Semiconductor Using Visible Light. *J. Am. Chem. Soc.* **2016**, *138* (15), 5159−5170.
(71) Maeda, K.; An, D.; Kumara Ranasinghe, C. S.; Uchiyama, T.; Kuriki, R.; Kanazawa, T.; Lu, D.; Nozawa, S.; Yamakata, A.; Uchimoto, Y.; Ishitani, O. Visible-Light CO $_2$ Reduction over a Ruthenium(II)-Complex/C $_3$ N $_4$ Hybrid Photocatalyst: The Promotional Effect of Silver Species. *J. Mater. Chem. A* **2018**, *6* (20), 9708−9715.
(72) Kuriki, R.; Yamamoto, M.; Higuchi, K.; Yamamoto, Y.; Akatsuka, M.; Lu, D.; Yagi, S.; Yoshida, T.; Ishitani, O.; Maeda, K. Robust Binding between Carbon Nitride Nanosheets and a Binuclear Ruthenium(II) Complex Enabling Durable, Selective CO $_2$ Reduction under Visible Light in Aqueous Solution. *Angew. Chem. Int. Ed* **2017**, *56* (17), 4867−4871.
(73) Sakakibara, N.; Kamogawa, K.; Miyoshi, A.; Maeda, K.; Ishitani, O. Synergetic Effect of Ligand Modification of a Ru(II) Complex Catalyst and Ag Loading for Constructing a Highly Active Hybrid Photocatalyst Using C_3N_4 for CO_2 Reduction. *Energy Fuels* **2024**, *38*, 2343.
(74) White, J. L.; Baruch, M. F.; Pander, J. E.; Hu, Y.; Fortmeyer, I. C.; Park, J. E.; Zhang, T.; Liao, K.; Gu, J.; Yan, Y.; Shaw, T. W.; Abelev, E.; Bocarsly, A. B. Light-Driven Heterogeneous Reduction of Carbon Dioxide: Photocatalysts and Photoelectrodes. *Chem. Rev.* **2015**, *115* (23), 12888−12935.
(75) Smieja, J. M.; Benson, E. E.; Kumar, B.; Grice, K. A.; Seu, C. S.; Miller, A. J. M.; Mayer, J. M.; Kubiak, C. P. Kinetic and Structural Studies, Origins of Selectivity, and Interfacial Charge Transfer in the Artificial Photosynthesis of CO. *Proc. Natl. Acad. Sci. U.S.A.* **2012**, *109* (39), 15646−15650.
(76) Morris, A. J.; Meyer, G. J.; Fujita, E. Molecular Approaches to the Photocatalytic Reduction of Carbon Dioxide for Solar Fuels. *Acc. Chem. Res.* **2009**, *42* (12), 1983−1994.
(77) Wang, C.; Xie, Z.; deKrafft, K. E.; Lin, W. Doping Metal-Organic Frameworks for Water Oxidation, Carbon Dioxide Reduction, and Organic Photocatalysis. *J. Am. Chem. Soc.* **2011**, *133* (34), 13445−13454.
(78) Wang, D.; Huang, R.; Liu, W.; Sun, D.; Li, Z. Fe-Based MOFs for Photocatalytic CO $_2$ Reduction: Role of Coordination Unsaturated Sites and Dual Excitation Pathways. *ACS Catal.* **2014**, *4* (12), 4254−4260.
(79) Wang, J.-L.; Wang, C.; Lin, W. Metal-Organic Frameworks for Light Harvesting and Photocatalysis. *ACS Catal.* **2012**, *2* (12), 2630−2640.
(80) Blake, A. J.; Champness, N. R.; Easun, T. L.; Allan, D. R.; Nowell, H.; George, M. W.; Jia, J.; Sun, X.-Z. Photoreactivity Examined through Incorporation in Metal−organic Frameworks. *Nature Chem.* **2010**, *2* (8), 688−694.
(81) Zhang, T.; Lin, W. Metal-Organic Frameworks for Artificial Photosynthesis and Photocatalysis. *Chem. Soc. Rev.* **2014**, *43* (16), 5982−5993.
(82) Lee, Y.; Kim, S.; Kang, J. K.; Cohen, S. M. Photocatalytic CO $_2$ Reduction by a Mixed Metal (Zr/Ti), Mixed Ligand Metal-Organic Framework under Visible Light Irradiation. *Chem. Commun.* **2015**, *51* (26), 5735−5738.
(83) Hod, I.; Sampson, M. D.; Deria, P.; Kubiak, C. P.; Farha, O. K.; Hupp, J. T. Fe-Porphyrin-Based Metal-Organic Framework Films as High-Surface Concentration, Heterogeneous Catalysts for Electrochemical Reduction of CO $_2$. *ACS Catal.* **2015**, *5* (11), 6302−6309.
(84) Liang, Y. T.; Vijayan, B. K.; Gray, K. A.; Hersam, M. C. Minimizing Graphene Defects Enhances Titania Nanocomposite-Based Photocatalytic Reduction of CO $_2$ for Improved Solar Fuel Production. *Nano Lett.* **2011**, *11* (7), 2865−2870.
(85) Neaţu, Ş.; Maciá-Agulló, J. A.; Concepción, P.; Garcia, H. Gold-Copper Nanoalloys Supported on TiO $_2$ as Photocatalysts for CO $_2$ Reduction by Water. *J. Am. Chem. Soc.* **2014**, *136* (45), 15969−15976.
(86) Liang, W.; Church, T. L.; Zheng, S.; Zhou, C.; Haynes, B. S.; D'Alessandro, D. M. Site Isolation Leads to Stable Photocatalytic Reduction of CO_2 over a Rhenium-Based Catalyst. *Chem.—Eur. J.* **2015**, *21* (51), 18576−18579.
(87) Choi, K. M.; Kim, D.; Rungtaweevoranit, B.; Trickett, C. A.; Barmanbek, J. T. D.; Alshammari, A. S.; Yang, P.; Yaghi, O. M. Plasmon-Enhanced Photocatalytic CO_2 Conversion within Metal-Organic Frameworks under Visible Light. *J. Am. Chem. Soc.* **2017**, *139* (1), 356−362.
(88) Ghosh, M.; Khan, S. N-Heterocyclic Carbenes Capped Metal Nanoparticles: An Overview of Their Catalytic Scope. *ACS Catal.* **2023**, *13* (14), 9313−9325.
(89) Kaur, G.; Thimes, R. L.; Camden, J. P.; Jenkins, D. M. Fundamentals and Applications of N-Heterocyclic Carbene Functionalized Gold Surfaces and Nanoparticles. *Chem. Commun.* **2022**, *58* (95), 13188−13197.
(90) Sherman, L. M.; Finley, M. D.; Borsari, R. K.; Schuster-Little, N.; Strausser, S. L.; Whelan, R. J.; Jenkins, D. M.; Camden, J. P. *N* -Heterocyclic Carbene Ligand Stability on Gold Nanoparticles in Biological Media. *ACS Omega* **2022**, *7* (1), 1444−1451.
(91) Cao, Z.; Kim, D.; Hong, D.; Yu, Y.; Xu, J.; Lin, S.; Wen, X.; Nichols, E. M.; Jeong, K.; Reimer, J. A.; Yang, P.; Chang, C. J. A Molecular Surface Functionalization Approach to Tuning Nanoparticle Electrocatalysts for Carbon Dioxide Reduction. *J. Am. Chem. Soc.* **2016**, *138* (26), 8120−8125.
(92) Jun, H.; Choi, S.; Lee, J. B.; Nam, Y. S. Plasmonic Heterostructure Functionalized with a Carbene-Linked Molecular Catalyst for Sustainable and Selective Carbon Dioxide Reduction. *ACS Appl. Mater. Interfaces* **2020**, *12* (30), 33817−33826.
(93) Wright, D.; Lin, Q.; Berta, D.; Földes, T.; Wagner, A.; Griffiths, J.; Readman, C.; Rosta, E.; Reisner, E.; Baumberg, J. J. Mechanistic Study of an Immobilized Molecular Electrocatalyst by in Situ Gap-Plasmon-Assisted Spectro-Electrochemistry. *Nat. Catal* **2021**, *4* (2), 157−163.
(94) Dey, A.; Silveira, V. R.; Vadell, R. B.; Lindblad, A.; Lindblad, R.; Shtender, V.; Görlin, M.; Sá, J. Exploiting Hot Electrons from a Plasmon Nanohybrid System for the Photoelectroreduction of CO_2. *Commun. Chem.* **2024**, *7* (1), 59.
(95) Falcone, P. M.; Hiete, M.; Sapio, A. Hydrogen Economy and Sustainable Development Goals: Review and Policy Insights. *Current Opinion in Green and Sustainable Chemistry* **2021**, *31*, 100506.
(96) Caiti, M.; Padovan, D.; Hammond, C. Continuous Production of Hydrogen from Formic Acid Decomposition Over Heterogeneous Nanoparticle Catalysts: From Batch to Continuous Flow. *ACS Catal.* **2019**, *9* (10), 9188−9198.
(97) Stephens, F. H.; Pons, V.; Tom Baker, R. Ammonia-Borane: The Hydrogen Source Par Excellence? *Dalton Trans.* **2007**, No. 25, 2613−2626.

https://doi.org/10.1021/acsnanoscienceau.4c00009
ACS Nanosci. Au 2024, 4, 273−289

(98) Enthaler, S.; Von Langermann, J.; Schmidt, T. Carbon Dioxide and Formic Acid—the Couple for Environmental-Friendly Hydrogen Storage? *Energy Environ. Sci.* **2010**, *3* (9), 1207.
(99) Ladomenou, K.; Natali, M.; Iengo, E.; Charalampidis, G.; Scandola, F.; Coutsolelos, A. G. Photochemical Hydrogen Generation with Porphyrin-Based Systems. *Coord. Chem. Rev.* **2015**, *304−305*, 38−54.
(100) Sheng, H.; Wang, J.; Huang, J.; Li, Z.; Ren, G.; Zhang, L.; Yu, L.; Zhao, M.; Li, X.; Li, G.; Wang, N.; Shen, C.; Lu, G. Strong Synergy between Gold Nanoparticles and Cobalt Porphyrin Induces Highly Efficient Photocatalytic Hydrogen Evolution. *Nat. Commun.* **2023**, *14* (1), 1528.
(101) Dey, A.; Mendalz, A.; Wach, A.; Vadell, R. B.; Silveira, V. R.; Leidinger, P. M.; Huthwelker, T.; Shtender, V.; Novotny, Z.; Artiglia, L.; Sá, J. Hydrogen Evolution with Hot Electrons on a Plasmonic-Molecular Catalyst Hybrid System. *Nat. Commun.* **2024**, *15* (1), 445.
(102) Gemenetzi, A.; Deligiannakis, Y.; Louloudi, M. Controlled Photoplasmonic Enhancement of H_2 Production *via* Formic Acid Dehydrogenation by a Molecular Fe Catalyst. *ACS Catal.* **2023**, *13* (14), 9905−9917.
(103) Gu, J.-Y.; Cai, Z.-F.; Wang, D.; Wan, L.-J. Single-Molecule Imaging of Iron-Phthalocyanine-Catalyzed Oxygen Reduction Reaction by *in Situ* Scanning Tunneling Microscopy. *ACS Nano* **2016**, *10* (9), 8746−8750.
(104) Jiang, S.; Chen, Z.; Chen, X.; Nguyen, D.; Mattei, M.; Goubert, G.; Van Duyne, R. P. Investigation of Cobalt Phthalocyanine at the Solid/Liquid Interface by Electrochemical Tip-Enhanced Raman Spectroscopy. *J. Phys. Chem. C* **2019**, *123* (15), 9852−9859.
(105) Nguyen, D.; Kang, G.; Chiang, N.; Chen, X.; Seideman, T.; Hersam, M. C.; Schatz, G. C.; Van Duyne, R. P. Probing Molecular-Scale Catalytic Interactions between Oxygen and Cobalt Phthalocyanine Using Tip-Enhanced Raman Spectroscopy. *J. Am. Chem. Soc.* **2018**, *140* (18), 5948−5954.

https://doi.org/10.1021/acsnanoscienceau.4c00009
ACS Nanosci. Au 2024, 4, 273−289